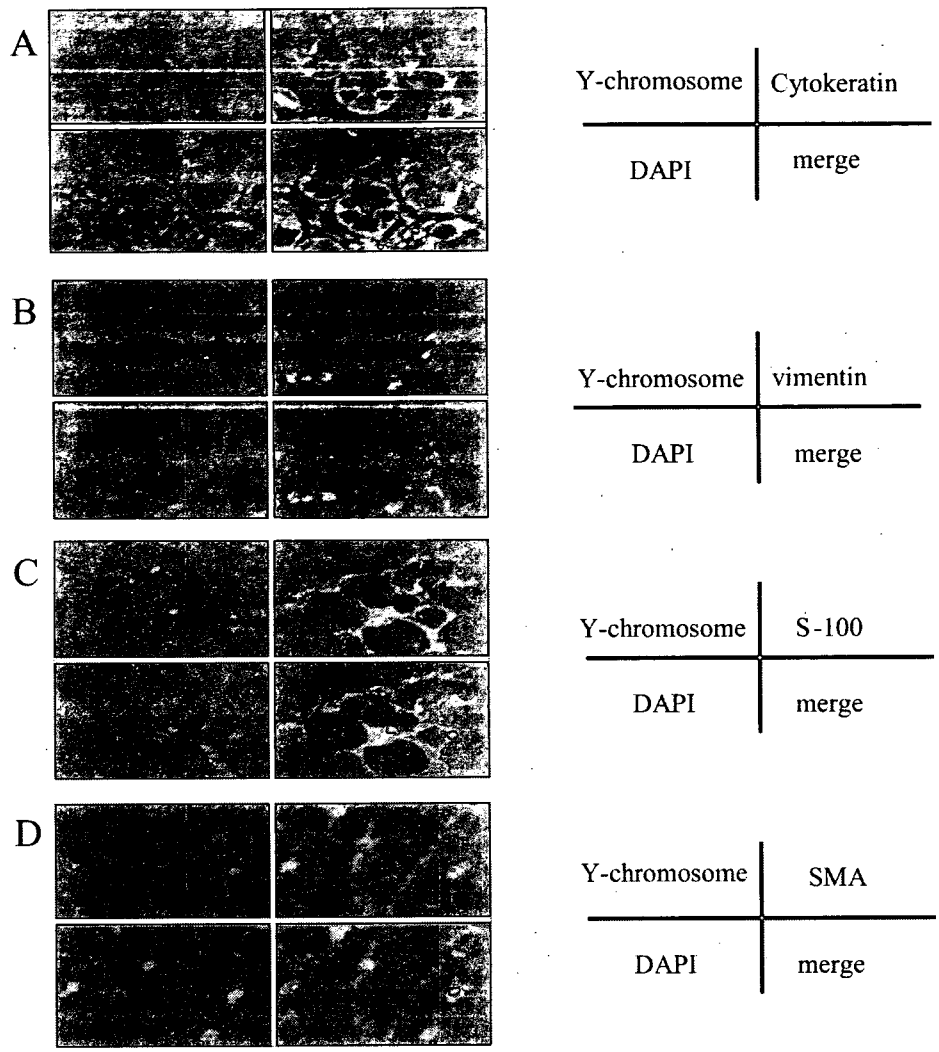

FIGURE 11. Immunofluorescent staining of Y-chromosome-positive cells. A: Y-chromosome-positive cells were not detected in epithelial cells that were stained by cytokeratin. B: Y-chromosome-positive cells were detected in fibroblast-like cells that were stained by vimentin. C: Y-chromosome-positive cells were detected in adipose tissues that were stained by S-100. D: Y-chromosome-positive cells were detected in the muscularis propria layer stained by SMA.

However, the decreases in the levels of IL-8 in the colonic tissue after the injection of ADSCs clearly indicate the wound-healing effects of ADSCs (Fig. 9), as also shown in the analyses of colon weight as an index of edema (Fig. 7). Furthermore, it is noted that the reduced activity of MPO observed in the colonic tissue confirms decreased infiltration of neutrophils and strengthens the effect of ADSCs. From these findings, it can be speculated that ADSCs prevent both the accumulation and the activation of neutrophils, thereby attenuating the neutrophil-dominant inflammation in colonic tissue caused by TNBS through the reduction of IL-8 levels that play a pivotal role in the accumulation of circulating leukocytes in inflammatory foci.[32] Furthermore, the effect of ADSCs might also be attributable to the anti-inflammatory effect of adiponectin, as shown in the previous study, in which adiponectin was found to exert its anti-inflammatory effect by inhibiting IL-8 production.[30] In addition, adiponectin promotes angiogenesis in response to tissue ischemia.[33] These data suggest that adiponectin secreted by ADSCs may also play a crucial role in TNBS-induced colitis.

FIGURE 10. Distribution of ADSCs in vivo by FISH. A: Fluorescence microscopy of colon 8 days after submucosal injection of 10^7 ADSCs (×10) showing almost healed to normal mucosa. B: Ulcer area undergoing healing. C–E: Distribution of ADSCs or ADSC-derived cells (Y-chromosome-positive cells) in mucosal (C), submucosal (D), and muscular layer (E). F: Y-chromosome-positive cells were counted in 3 low-magnification fields per rat colon 8 days after submucosal injection of ADSCs. Columns and bars represent the means ± SDs of 10 rats ($^*P < 0.001$).

As shown in Figure 10, cells derived from ADSCs, defined by Y-FISH, were detected in the mucosal layer under the basal membrane, the submucosal layer around the vessel, and the muscle layer; they were especially observed in the

area of inflammation, such as the ulcer edge. They could be thought to differentiate into fibroblast-lineage (vimentin-positive cells), adipocyte-lineage (S-100-positive cells), and muscle-lineage cells (SMA-positive cells) when immunohistochemically examined. However, they were not detected in the epithelial layer, indicating that ADSCs (submucosally injected) did not differentiate into epithelial-lineage or neural-lineage cells, even though they differentiated into various lineage cells in vitro (Figs. 4 and 5). This is in contrast with the findings that bone marrow MSCs were detected in the epithelium of the stomach and intestine[34] and differentiated into neural cells[35] and that MSCs in bone marrow seem to be more primitive than ADSCs. Therefore, our results indicate that although ADSCs have the potential to differentiate into various lineage cells in vitro, ADSCs in vivo can differentiate into mesodermal lineage cells.

Examination in vitro showed that collectively, ADSCs have multiple differentiation ability and secrete growth factors such as VEGF and HGF in large quantities and also produce adiponectin. Therefore, although we have not measured the tissue levels of these growth factors after the injection of ADSCs, it is highly feasible that ADSCs injected in vivo (1×10^7 cells) produce them and that these soluble factors might be responsible for the regeneration of the injured regions observed in the TNBS-induced colitis. Moreover, some ADSCs may differentiate into the various components of the colon, such as smooth muscles, fibroblasts, and myofibroblasts. These mesodermal cells are essential for facilitating the regeneration of epithelial cells. Furthermore, ADSCs improved TNBS-induced colitis by ameliorating colonic injury induced by proinflammatory cytokines.

Importantly, the safety of high-dose lipoaspiration to obtain ADSCs in humans was already established,[36] and thus ADSCs are a viable therapeutic option for amelioration of Crohn's disease or IBD by repairing injured intestinal mucosa. If the number of ADSCs obtained from the subcutaneous adipose tissues of the abdomens of patients themselves is enough to use for the cell therapy, ADSCs can be immediately applicable without cell culture, and the remaining ADSCs can be kept by cryopreservation for future use when a fistula recurs. In addition, treatment via endoscopy is considered a general and established method, thereby submucosally injecting ADSCs without an operation. It is feasible that in vitro cultured ADSCs inoculated into the submucosa are transformed into tumors. Therefore, we have to examine this possibility for a long life span after the treatment, and these types of experiments are now under investigation.

In conclusion, ADSCs can accelerate the regeneration of injured regions, and HGF, VEGF, and adiponectin produced by ADSCs might be responsible for the regeneration.

ACKNOWLEDGMENTS

The authors thank Mr. Hilary Eastwick-Field, Mr. Brian O'Flaherty, and Ms. K. Ando for their help in the preparation of the manuscript.

REFERENCES

1. Katz AJ, Tholpady A, Tholpady SS, et al. Cell surface and transcriptional characterization of human adipose-derived adherent stromal (hADAS) cells. *Stem Cells.* 2005;23:412–423.
2. Strem BM, Hicok KC, Zhu M, et al. Multipotential differentiation of adipose tissue-derived stem cells [review]. *Keio J Med.* 2005;54:132–141.
3. De Ugarte DA, Morizono K, Elbarbary AS, et al. Comparison of multi-lineage cells from human adipose tissue and bone marrow. *Cells Tissues Organs.* 2004;174:101–109.
4. Lee RH, Kim B, Choi I, et al. Characterization and expression analysis of mesenchymal stem cells from human bone marrow and adipose tissue. *Cell Physiol Biochem.* 2004;14:311–324.
5. Garcia-Olmo D, Garcia-Arranz M, Herreros D, et al. A phase I clinical trial of the treatment of Crohn's fistula by adipose mesenchymal stem cell transplantation. *Dis Colon Rectum.* 2005;48:1416–1423.
6. Schrepfer S, Deuse T, Reichenspurner H, et al. Stem cell transplantation: the lung barrier. *Transplant Proc.* 2007;39:573–576.
7. Kern S, Eichler H, Stoeve J, et al. Comparative analysis of mesenchymal stem cells from bone marrow, umbilical cord blood, or adipose tissue. *Stem Cells.* 2006;24:1294–1301.
8. Woodbury D, Schwarz EJ, Prockop DJ, et al. Adult rat and human bone marrow stromal cells differentiate into neurons. *J Neurosci Res.* 2000; 61:364–370.
9. Zuk PA, Zhu M, Ashjian P, et al. Human adipose tissue is a source of multipotent stem cells, *Mol Biol Cell.* 2002;13:4279–4295.
10. Brzoska M, Geiger H, Gauer S, Baer P. Epithelial differentiation of human adipose tissue-derived adult stem cells. *Biochem Biophys Res Commun.* 2005;330:142–150.
11. Morris GP, Beck PL, Herridge MS, et al. Hapten-induced model of chronic inflammation and ulceration in the rat colon. *Gastroenterology.* 1989;96:795–803.
12. Macpherson BR, Pfeiffer CJ. Experimental production of diffuse colitis in rats. *Digestion.* 1978;17:135–150.
13. Tsune I, Ikejima K, Hirose M, et al. Dietary glycine prevents chemical-induced experimental colitis in the rat. *Gastroenterology.* 2003;125: 775–785.
14. Krawisz JE, Sharon P, Stenson WF. Quantitative assay for acute intestinal inflammation based on myeloperoxidase activity. Assessment of inflammation in rat and hamster models. *Gastroenterology.* 1984;87: 1344–1350.
15. Javazon EH, Colter DC, Schwarz EJ, et al. Rat marrow stromal cells are more sensitive to plating density and expand more rapidly from single-cell-derived colonies than human marrow stromal cells. *Stem Cells.* 2001;19:219–225.
16. Yoshimura H, Muneta T, Nimura A, et al. Comparison of rat mesenchymal stem cells derived from bone marrow, synovium, periosteum, adipose tissue, and muscle. *Cell Tissue Res.* 2007;327:449–462.
17. Ashjian PH, Elbarbary AS, Edmonds B, et al. In vitro differentiation of human processed lipoaspirate cells into early neural progenitors. *Plast Reconstr Surg.* 2003;111:1922–1931.
18. Brzoska M, Geiger H, Gauer S, et al. Epithelial differentiation of human adipose tissue-derived adult stem cells. *Biochem Biophys Res Commun.* 2005;330:142–150.
19. Gimble JM, Guilak F. Adipose-derived adult stem cells: isolation, characterization, and differentiation potential. *Cytotherapy.* 2003;5:362–369.
20. Rehman J, Traktuev D, Li J, et al. Secretion of angiogenic and antiapoptotic factors by human adipose stromal cells. *Circulation.* 2004; 109:1292–1298.
21. Zvonic S, Lefevre M, Kilroy G, et al. Secretome of primary cultures of human adipose-derived stem cells: modulation of serpins by adipogenesis. *Mol Cell Proteomics.* 2007;6:18–28.
22. Van Belle E, Witzenbichler B, Chen D, Silver et al. Potentiated angiogenic effect of scatter factor/hepatocyte growth factor via induction of

vascular endothelial growth factor: the case for paracrine amplification of angiogenesis. *Circulation.* 1998;97:381–390.
23. Yaekashiwa M, Nakayama S, Ohnuma K, et al. Simultaneous or delayed administration of hepatocyte growth factor equally represses the fibrotic changes in murine lung injury induced by bleomycin. A morphologic study. *Am J Respir Crit Care Med.* 1997;156:1937–1944.
24. Matsuda Y, Matsumoto K, Yamada A, et al. Preventive and therapeutic effects in rats of hepatocyte growth factor infusion on liver fibrosis/cirrhosis. *Hepatology.* 1997;26:81–89.
25. Xin X, Yang S, Ingle G, et al. Hepatocyte growth factor enhances vascular endothelial growth factor-induced angiogenesis in vitro and in vivo. Am J Pathol. 2001;158:1111–1120.
26. Numata M, Ido A, Moriuchi A, et al. Hepatocyte growth factor facilitates the repair of large colonic ulcers in 2,4,6-trinitrobenzene sulfonic acid-induced colitis in rats. *Inflamm Bowel Dis.* 2005;11:551–558.
27. Ouchi N, Kihara S, Arita Y, et al. Novel modulator for endothelial adhesion molecules: adipocyte-derived plasma protein adiponectin. *Circulation.* 1999;100:2473–2476.
28. Wulster-Radcliffe MC, Ajuwon KM, Wang J, et al. Adiponectin differentially regulates cytokines in porcine macrophages. *Biochem Biophys Res Commun.* 2004,;316:924–929.
29. Wolf AM, Wolf D, Rumpold H, Enrich B, Tilg H. Adiponectin induces the anti-inflammatory cytokines IL-10 and IL-1RA in human leukocytes. *Biochem Biophys Res Commun.* 2004;323:630–635.
30. Nishihara T, Matsuda M, Araki H, et al. Effect of adiponectin on murine colitis induced by dextran sulfate sodium. *Gastroenterology.* 2006;131:853–861.
31. Yokota T, Oritani K, Takahashi I, et al. Adiponectin, a new member of the family of soluble defense collagens, negatively regulates the growth of myelomonocytic progenitors and the functions of macrophages. *Blood.* 2000;96:1723–1732.
32. Pender SL, Chance V, Whiting CV, et al. Systemic administration of the chemokine macrophage inflammatory protein 1alpha exacerbates inflammatory bowel disease in a mouse model. *Gut.* 2005;54:1114–1120.
33. Shibata R, Ouchi N, Kihara S, et al. Adiponectin stimulates angiogenesis in response to tissue ischemia through stimulation of amp-activated protein kinase signaling. *J Biol Chem.* 2004;279:28670–28674.
34. Semont A, Francois S, Mouiseddine M, et al. Mesenchymal stem cells increase self-renewal of small intestinal epithelium and accelerate structural recovery after radiation injury. *Adv Exp Med Biol.* 2006;585:19–30.
35. Sanchez-Ramos J, Song S, Cardozo-Pelaez F, et al. Adult bone marrow stromal cells differentiate into neural cells in vitro. *Exp Neurol.* 2002;164:247–256.
36. Cardenas-Camarena L. Lipoaspiration and its complications: a safe operation. *Plast Reconstr Surg.* 2003;112:1435–1441; discussion 1442–1443.

Y. Ito, T. Kanai, T. Totsuka, R. Okamoto, K. Tsuchiya, Y. Nemoto, A. Yoshioka, T. Tomita, T. Nagaishi, N. Sakamoto, T. Sakanishi, K. Okumura, H. Yagita and M. Watanabe
Am J Physiol Gastrointest Liver Physiol 294:199-207, 2008. First published Oct 25, 2007;
doi:10.1152/ajpgi.00286.2007

You might find this additional information useful...

This article cites 30 articles, 10 of which you can access free at:
http://ajpgi.physiology.org/cgi/content/full/294/1/G199#BIBL

Updated information and services including high-resolution figures, can be found at:
http://ajpgi.physiology.org/cgi/content/full/294/1/G199

Additional material and information about ***AJP - Gastrointestinal and Liver Physiology*** can be found at:
http://www.the-aps.org/publications/ajpgi

This information is current as of February 20, 2008 .

AJP - Gastrointestinal and Liver Physiology publishes original articles pertaining to all aspects of research involving normal or abnormal function of the gastrointestinal tract, hepatobiliary system, and pancreas. It is published 12 times a year (monthly) by the American Physiological Society, 9650 Rockville Pike, Bethesda MD 20814-3991. Copyright © 2005 by the American Physiological Society. ISSN: 0193-1857, ESSN: 1522-1547. Visit our website at http://www.the-aps.org/.

Am J Physiol Gastrointest Liver Physiol 294: G199–G207, 2008.
First published October 25, 2007; doi:10.1152/ajpgi.00286.2007.

Blockade of NKG2D signaling prevents the development of murine CD4 T cell-mediated colitis

Y. Ito,[1] T. Kanai,[1] T. Totsuka,[1] R. Okamoto,[1] K. Tsuchiya,[1] Y. Nemoto,[1] A. Yoshioka,[1] T. Tomita,[1] T. Nagaishi,[1] N. Sakamoto,[1] T. Sakanishi,[2] K. Okumura,[3] H. Yagita,[3] and M. Watanabe[1]

[1]*Department of Gastroenterology and Hepatology, Graduate School, Tokyo Medical and Dental University, Tokyo; and* [2]*Division of Cell Biology and* [3]*Department of Immunology, Juntendo University School of Medicine, Tokyo, Japan*

Submitted 23 June 2007; accepted in final form 17 October 2007

Ito Y, Kanai T, Totsuka T, Okamoto R, Tsuchiya K, Nemoto Y, Yoshioka A, Tomita T, Nagaishi T, Sakamoto N, Sakanishi T, Okumura K, Yagita H, Watanabe M. Blockade of NKG2D signaling prevents the development of murine CD4 T cell-mediated colitis. *Am J Physiol Gastrointest Liver Physiol* 294: G199–G207, 2008. First published October 25, 2007; doi:10.1152/ajpgi.00286.2007.—It has been recently demonstrated that NKG2D is an activating costimulatory receptor on natural killer (NK) cells, natural killer T (NKT) cells, activated CD8 T cells, and T cells, which respond to cellular stress, such as inflammation, transformation, and infection. Here we show that intestinal inflammation in colitic SCID mice induced by adoptive transfer of CD4 CD45RB^{high} T cells is characterized by significant increase of CD4 NKG2D T cells and constitutive expression of NKG2D ligands, such as H60, Mult-1, and Rae-1, by lamina propria CD11c dendritic cells. Furthermore, treatment with nondepleting and neutralizing anti-NKG2D MAb after transfer of CD4 CD45RB^{high} T cells into SCID mice significantly suppressed wasting disease with colitis, abrogated leukocyte infiltration, and reduced production of IFN- by lamina propria CD4 T cells. These findings demonstrate that NKG2D signaling pathway is critically involved in CD4 T cell-mediated disease progression and suggest a new therapeutic target for inflammatory bowel diseases.

NKG2D; CD4 T cells; chronic colitis; inflammatory bowel disease

INFLAMMATORY BOWEL DISEASES (IBDs), such as Crohn's disease and ulcerative colitis, are chronic inflammatory diseases characterized by massive infiltration of activated effector-memory CD4 T cells, macrophages, and dendritic cells in the inflamed mucosa (3, 24). Although their etiology remains unclear, it has been shown that production of proinflammatory cytokines by infiltrating activated CD4 T cells and macrophages plays a critical role in the pathogenesis of IBD (2, 4, 10, 13).

It is well known that the activation of CD4 T cells requires two distinct signals: signal 1 derived from the interaction between the T cell receptor (TCR) and peptide-major histocompatibility complex (MHC), and signal 2, the costimulatory signal, derived from the interaction between costimulatory molecules of CD28 family on CD4 T cells and their ligands of the B7 family on antigen-presenting cells (APC) (7, 8, 16). In addition to the CD28/B7 family pathway (27, 28), accumulating evidence shows that many other costimulatory systems, such as the TNF- /TNF- receptor family pathway, are also involved in the pathogenesis of IBDs and animal models of chronic colitis (18, 21, 26, 29).

NKG2D was first shown as a novel costimulatory molecule expressed on NK cells, which was also demonstrated to be expressed on CD8 T cells, T cells, and NKT cells that have cytotoxic activity (23, 25). In CD8 T cells, NKG2D is expressed on activated effector-memory, but not resting naive, CD8 T cells. The ligands of NKG2D are poorly expressed on normal cells but are upregulated on stressed, transformed, or infected cells (23, 25). To date, it has been reported that mouse NKG2D ligands include the retinoic acid early inducible (Rae)-1 family of proteins (6), the minor histocompatibility antigen H60 (20), and murine UL-16-binding protein-like transcript (Mult)-1 glycoprotein (5). It has been demonstrated that the activation via NKG2D receptor can enhance negative signals by MHC class I-specific NK cell inhibitory receptors (9, 15).

Although it had been believed that both human and mouse CD4 T cells do not express NKG2D, recent studies have suggested that NKG2D expression could be observed in a fraction of CD4 T cells residing in the peripheral blood and synovial tissue from patients with rheumatoid arthritis (12). To characterize the role of NKG2D molecule expressed on colitogenic CD4 effector-memory T cells in the development of colitis, we utilized a Th1-type CD4 T-cell-mediated Crohn's disease-like colitis model induced in SCID mice by adoptive transfer of CD4 CD45RB^{high} T cells (27). We here demonstrate that the lamina propria (LP) CD4 CD44^{high} memory T cells in inflamed mucosa express NKG2D. Furthermore, we show that neutralizing anti-mouse NKG2D MAb suppressed the development of colitis.

MATERIALS AND METHODS

Animals. Six- to 8-wk-old female C.B-17 SCID mice and BALB/c mice were purchased from Japan Clea (Tokyo, Japan). Mice were maintained under specific pathogen-free conditions in the Animal Care Facility at Tokyo Medical and Dental University. Donors and littermate recipients were used at 6–12 wk of age. All experiments were approved by the regional animal study committees.

Antibodies. The anti-murine NKG2D MAb (HMG2D, hamster IgG) was generated by immunizing an American hamster with mouse NKG2D-Fc fusion protein (R&D Systems, Minneapolis, MN). This MAb inhibited the binding of NKG2D-Fc to Rae-1 transfectants and blocked the killing of Rae-1 transfectants by NK cells but did not activate NK cells in vitro or deplete NK cells in vivo. We confirmed that this activity of HMG2D was comparable to another clone of anti-NKG2D MAb, CX5 (17) (data not shown). The following MAbs were obtained from BD Pharmingen (San Diego, CA) and used for purification of cell populations and flow cytometric analysis: Fc R

Address for reprint requests and other correspondence: T. Kanai, MD, Dept. of Gastroenterology and Hepatology, Tokyo Medical and Dental Univ., 1-5-45 Yushima, Bunkyo-ku, Tokyo 113-8519, Japan (e-mail: taka.gast@tmd.ac.jp).

The costs of publication of this article were defrayed in part by the payment of page charges. The article must therefore be hereby marked "*advertisement*" in accordance with 18 U.S.C. Section 1734 solely to indicate this fact.

0193-1857/08 $8.00 Copyright © 2008 the American Physiological Society

(CD16/CD32)-blocking MAb (2.4G2); FITC-, phycoerythrin (PE)-, and phycoerythrin-cyanin5 (PECy5)-conjugated anti-mouse CD4 (RM4-5); FITC-conjugated anti-mouse CD3 (145-2C11); FITC-conjugated anti-mouse CD45RB (16A); FITC-conjugated anti-mouse CD11b (M1/70); FITC-conjugated anti-mouse CD11c (HL3); FITC-conjugated anti-mouse DX5 (DX5); APC-conjugated anti-mouse CD28 (37.51); FITC-conjugated anti-mouse inducible T-cell costimulator (ICOS) (C398.4); FITC-conjugated anti-mouse PD-1 (RMP1-30); PE-conjugated streptavidin; biotin-conjugated rat IgG2; PE-conjugated mouse IgG; and PE-conjugated rat IgG.

In vivo experimental design. Colitis was induced in SCID mice by adoptive transfer of CD4 CD45RB^{high} T cells as previously described (27). CD4 T cells were isolated from splenic mononuclear cells from BALB/c mice by using the anti-CD4 (L3T4) MACS magnetic separation system (Miltenyi Biotec, Auburn, CA) according to the manufacturer's instruction. Enriched CD4 T cells were then labeled with PE-conjugated anti-mouse CD4 MAb (RM4-5) and FITC-conjugated anti-CD45RB MAb (16A) and sorted into CD45RB^{high} (highest staining 30%) and CD45RB^{low} (lowest staining 30%) fractions on a FACS Vantage (Becton Dickinson, Sunnyvale, CA). Each SCID mouse was injected with 200 l ip of PBS containing 3 10^5 cells of CD4 CD45RB^{high} T cells. These mice were then administered with 250 g ip of anti-NKG2D MAb in 250 l PBS three times per week, starting at the day of T cell transfer, over a period of 7 wk in the preventive protocol. An equivalent amount of control hamster IgG (Sigma-Aldrich, St. Louis, MO) was administered in control mice. Negative control SCID mice were also transferred with a mixture of 3 10^5 CD4 CD45RB^{high} T cells and 3 10^5 CD4 CD45RB^{low} T cells.

Disease monitoring and clinical scoring. Mice were weighed and monitored for appearance and signs of soft stool and diarrhea once a week. Clinical score (27) was assessed at 7–8 wk after T cell transfer as the sum of three parameters as follows: hunching and wasting, 0 or 1; colon thickening, 0–3 (0, no colon thickening; 1, mild thickening; 2, moderate thickening; 3, extensive thickening); and stool consistency, 0–3 (0, normal beaded stool; 1, soft stool; 2, diarrhea; 3, gross bloody stool).

Histological examination. Tissue samples were fixed in 6% phosphate-buffered formalin. Paraffin-embedded sections (5 m) were stained with hematoxylin and eosin. Three tissue samples from the proximal, middle, and distal parts of the colon were prepared. The sections were analyzed without prior knowledge of the type of treatment. The area most affected was graded by the number and severity of lesions. The mean degree of inflammation in the colon was calculated via a modification of a previously described scoring system (19).

Immunohistochemistry. For immunohistochemistry, colonic samples were snap-frozen in liquid nitrogen and stored at 80°C. Cryostat sections (5 m) were fixed in 4% paraformaldehyde and detection of mouse CD4 and NKG2D was performed by the avidin-biotin complex method. Briefly, after blocking, the sections were incubated with primary rat anti-mouse NKG2D MAb (clone 191004, R&D Systems) and goat anti-mouse CD4 MAb (AF554, R&D Systems), followed by biotin-conjugated goat anti-rat IgG (1:200, Vector Laboratories, Burlingame, CA) and biotin-conjugated rabbit anti-goat IgG (1:200, Vector Laboratories). The deposition of the biotin on tissue sections was detected by streptavidin-biotinylated horseradish peroxidase complex (Vectastain ABC kit, Vector) and diaminobenzidine. Then the sections were counterstained with hematoxylin.

To assess the colocalization of CD4 and NKG2D on colitic LP CD4 T cells, we further performed an immunofluorescent staining experiment. Sections were incubated with rat anti-mouse NKG2D MAb (clone 191004) and goat anti-mouse CD4 MAb (AF554), followed by biotin-conjugated goat anti-rat IgG and amino acid polymer conjugated with rabbit anti-goat IgG and peroxidase (NICHIREI Bioscience, Tokyo, Japan). The samples were then incubated with Alexa 488-conjugated tyramide at a 1:100 dilution (Molecular Probes, Eugene, OR) for detection of CD4 and streptavidin-Alexa Fluor 594 conjugate (Molecular Probes) for detection of NKG2D. Cell nuclei were counterstained with DAPI (Molecular Probes). Stained sections were examined by a BioZERO BZ8000 (KEYENCE, Osaka, Japan).

Preparation of LP lymphocytes and splenocytes. For the isolation of LP lymphocytes from the colon, the entire length of intestine was opened longitudinally, washed with PBS, and cut into small pieces. The dissected mucosa was incubated two times with Ca^2 - and Mg^2 -free Hanks' balanced salt solution containing 1 mM dithiothreitol (Sigma-Aldrich) for 30 min each to remove mucus. The supernatants containing intraepithelial cells and epithelial cells were removed. Collected tissues were treated with 3 mg/ml collagenase A (Worthington Biomedical, Freehold, NJ) and 0.01% DNase (Worthington) in RPMI 1640 medium for 2 h. The cells were pelleted two times through a 40% isotonic Percoll solution and then further purified by Ficoll-Hypaque density gradient centrifugation (40%/75%). LP CD4 T cells were obtained by positive selection via the anti-CD4 (L3T4) MACS magnetic separation system. The cells were 95% CD4 when analyzed by flow cytometry. Splenic mononuclear cells were obtained from the same animals by mechanical dissociation of the spleen followed by Ficoll-Hypaque density gradient centrifugation.

Flow cytometry. Isolated LP mononuclear cells or splenocytes were preincubated with Fc R-blocking MAb (2.4G2) for 20 min, followed by incubation with FITC-, PE-, or biotin-labeled MAb for 30 min on ice. Biotinylated antibodies were detected with PE- or CyChrome-streptavidin. Standard two- or three-color flow cytometric analyses were obtained by use of the FACS Calibur using CellQuest software. Background fluorescence was assessed by staining with control irrelevant isotype-matched MAbs.

Quantitative RT-PCR. Whole colon from colitic SCID mice and age-matched normal BALB/c mice were opened longitudinally, washed, and cut into pieces, then homogenized three times by homogenizer. Each cell population of LP cells from colitic mice was isolated by the anti-CD4, CD11b, or CD11c MACS magnetic separation (Miltenyi Biotec). Colonic intestinal epithelial cells (IECs) were also isolated as previously described (11). Total RNA was extracted using ISOGEN reagent (Nippon Gene, Tokyo, Japan). Aliquots of 3 g of total RNA were used for complementary DNA synthesis in 14 l of reaction volume by using random primers. One l of complementary DNA was amplified with 12.5 l of SYBR Green PCR master mix (Qiagen, Hilden, Germany) in a 25- l reaction volume. Sense and antisense primers for the amplification of each gene were as follows: sense H60, 5 -GTGTGATGACGATTTGTTGAG-3 and antisense H60, 5 -ATTGATGGATTCTGGGCCATA-3 ; sense Mult-1, 5 -CTCATAGGAACAGCATGA-3 and an-

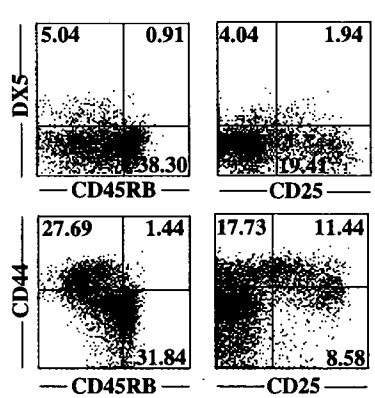

Fig. 1. DX5 NKT cells do not reside in splenic CD4 CD45RB^{high} cell population. Phenotypic characterization of splenic CD4 CD45RB^{high} cells and CD4 CD25 cells in terms of expression of DX5 and CD44. Data represent FACS profiles from 3 independent experiments.

tisense Mult-1 5 -TCCTGTGAAATGTTTGTC-3 ; sense isoforms of retinoic acid early transcript 1 (Rae-1) molecules (Rae-1), 5 -ATAATGGATCCATGGCCAAGGCAGCAGTGACCAA-3 and antisense Rae-1 , 5 -ATATTATAGCGGCCGCTCACATCG-CAAATGCAAATGCAAATAAT-3 ; and sense glyceraldehyde-3-phosphate dehydrogenase (G3PDH), 5 -TGAAGGTCGGTGTGAA-CGGATTTGGC-3 and antisense G3PDH, 5 -CATGTAGGC-CATGAGGTCCACCAC-3 . Analysis was performed on Applied Biosystems 7500 real-time PCR system (Applied Biosystems, Foster City, CA). mRNA level of each ligand was normalized by the corresponding level of G3PDH mRNA.

Cytokine production assay. To measure cytokine production, LP CD4 T cells (1 10^5) were cultured in 200 l of culture medium at 37°C in a humidified atmosphere containing 5% CO_2 in 96-well plates (Costar, Cambridge, MA) precoated with 5 g/ml of hamster anti-mouse CD3ε MAb (145-2C11, BD Pharmingen) and 2 g/ml of

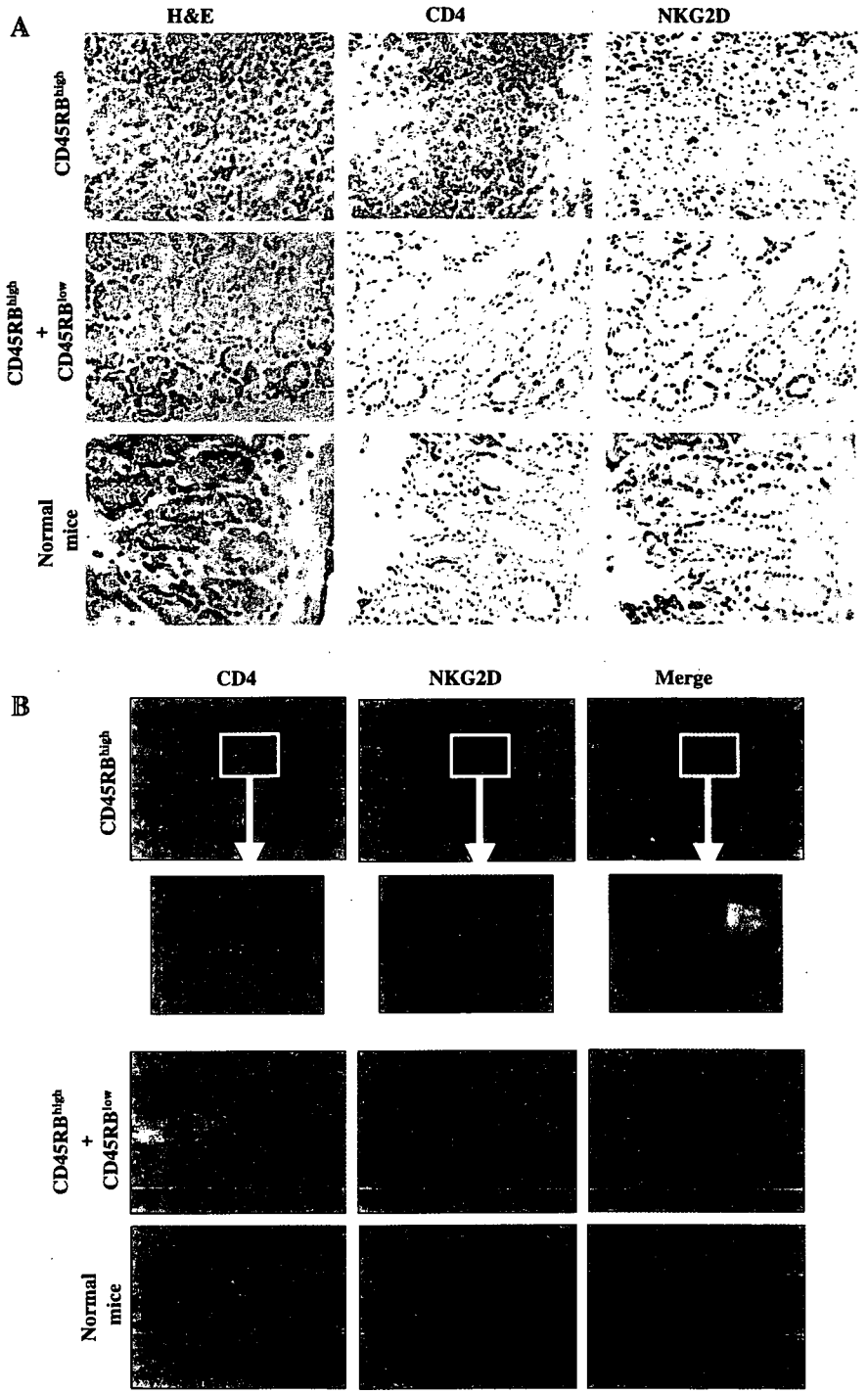

Fig. 2. Expression of NKG2D by colitic LP CD4 T cells. *A*: frozen serial sections of the colons from colitic SCID mice transferred with CD4 CD45RB^{high} T cells, noncolitic SCID mice transferred with a mixture of CD4 CD45RB^{high} T cells and CD4 CD45RB^{low} T cells, and age-matched normal BALB/c mice were stained with anti-CD4 or anti-NKG2D MAb, or hematoxylin and eosin (H&E). Representative of 5 separate samples in each group. Original magnification 100. *B*: fluorescence image of CD4 and NKG2D. Frozen sections were doubly stained with anti-CD4 in green and anti-NKG2D MAbs in red. Representative of 5 separate samples in each group. Original magnification 60.

hamster anti-mouse CD28 MAb (37.51, BD Pharmingen) in PBS overnight at 4°C. Culture supernatants were collected after 48 h of culture and assayed for cytokine production. Cytokine concentrations were measured by mouse Cytokine CBA kit (BD Biosciences, San Jose, CA) per the manufacturer's recommendation.

Statistical analysis. The results were expressed as means SE. Groups of data were compared by Mann-Whitney *U*-test. Differences were considered to be statistically significant when *P* 0.05.

RESULTS

Expression of NKG2D in CD4 CD45RB^{high} T cell-transferred SCID mice. To investigate whether interactions between NKG2D and its ligands are involved in the development of chronic colitis, we used a murine model of chronic colitis induced in C.B-17 SCID mice by adoptive transfer of CD4 CD45RB^{high} T cells of normal BALB/c mice (27), where high refers to the brightest staining 30% fluorescence intensity of CD4 T cells. In this colitis model, CD8 T cells and B cells are absent as we transferred only CD4 CD45RB^{high} T cells into SCID mice lacking both T and B cells. However, it should be noted that CD4 donor population contains a small number of CD4 NKT cells that can express inducible NKG2D in addition to a majority of conventional CD4 TCR T cells. To precisely evaluate this issue, we performed three-color flow cytometry analysis of the cells that were prepared for transfer. As shown in Fig. 1, a small number of DX5 cells were surely observed in the CD4 CD45RB$^{low\text{-}moderate}$ population, but not in the CD4 CD45RB^{high} population. Furthermore, we found that CD4 CD25 cells, which are another population of donor cells commonly used to induce colitis in SCID mice (17), contained substantial number of DX5 cells (Fig. 1, *top*). Furthermore, almost all CD4 CD45RB^{high} T cells had CD44^{low} (low refers to the dullest 30% CD4 T cells, and moderate refers to the intermediate staining populations between the previous two populations) naive phenotype, whereas CD4 CD25 T cells contained substantial numbers of CD44^{high} memory T cells along with CD44^{low} naive T cells (Fig. 1, *bottom*). Thus we decided to use CD4 CD45RB^{high} T cells as donor cells to assess the possible role of NKG2D expression by conventional CD4 T cells in the development of colitis, so as to exclude the involvement of NKT cells.

After adoptive transfer of CD4 CD45RB^{high} cells, the recipient mice manifested weight loss from 3 wk after transfer and clinical symptoms of colitis such as diarrhea with increased mucus in the stool, anorectal prolapse, and hunched posture by 6 wk (data not shown). The colons from these mice were enlarged and had a greatly thickened wall due to severe colonic inflammation (Fig. 2*A*, *left*). In contrast, when transferred with a mixture of CD4 CD45RB^{high} and CD4 CD45RB^{low} cells, the recipient mice did not develop colitis at all as well as control BALB/c mice (Fig. 2*A*, *left*).We then examined the expression of CD4 and NKG2D in this model by immunohistochemistry. Colonic samples were obtained from colitic SCID mice transferred with CD4 CD45RB^{high} cells, noncolitic SCID mice transferred with CD4 CD45RB^{high} and CD4 CD45RB^{low} cells at 6 wk after the transfer, and age-matched BALB/c mice as a control. Figure 2*A* shows that CD4 T cells were markedly increased in the inflamed mucosa of colitic SCID mice transferred with CD4 CD45RB^{high} T cells (Fig. 2*A*, *middle*), but not in noncolitic SCID mice transferred with CD4 CD45RB^{high} and CD4 CD45RB^{low} T cells or normal mice. The majority of CD4 T cells in colitic SCID mice located in the LP and submucosa, but some of the cells appeared to locate also in the tunica muscularis and subserosa. Of note, in colitic mice, the distribution of NKG2D cells were scattered within the location of CD4 T cells (Fig. 2*A*, *right*), suggesting that NKG2D was expressed by a part of colitic CD4 LP T cells. In contrast, a small number of CD4 T cell were indeed found in the LP of noncolitic SCID mice transferred with CD4 CD45RB^{high} and CD4 CD45RB^{low} T cells and in normal mice, but expression of NKG2D could never be detected on these normal LP CD4 T cells (Fig. 2*A*, *middle* and *right*). To further confirm that NKG2D is expressed on CD4 T cells in colitic LP, we performed a double-staining experiment by fluorescent immunostaining. As shown in Fig. 2*B*, NKG2D was surely expressed by a part of CD4 T cells in colitic mice. In contrast, a small number of CD4 T cell showed scattered distribution in the LP of noncolitic SCID or normal BALB/c mice, but NKG2D was not detected in these mice.

To further confirm the expression of NKG2D on CD4 T cells in colitic mice, we next performed two-color flow cytom-

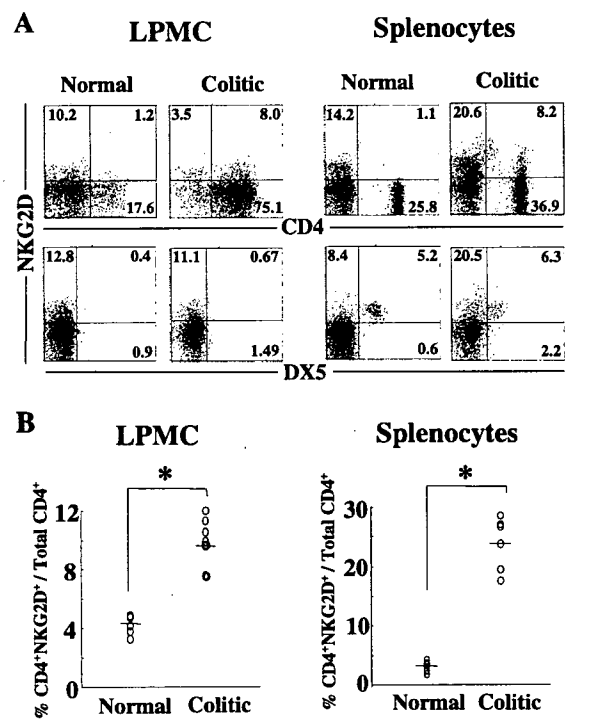

Fig. 3. NKG2D is expressed on lamina propria (LP) and splenic CD4 T cells in colitic mice. Expression of NKG2D on splenic and LP CD4 and DX5 cells in colitic SCID mice (6 wk after transfer) and age-matched normal BALB/c mice. *A*: freshly isolated cells from colitic mice and normal BALB/c mice were stained with anti-NKG2D MAb, anti-CD4, or DX5 MAb. Samples were analyzed by flow cytometry. Lymphocytes were identified by characteristic forward angle and side scatter profiles. Data are displayed as dotted plot (4-decade log scale), and quadrant markers were positioned to include 98% of control Ig-stained cells in the *bottom left*. Percentages in each quadrant are indicated. Data are representative of 6 mice in each group. *B*: expression of NKG2D on LP and splenic CD4 T cells from colitic mice is significantly increased compared with that on the paired samples from normal mice. Data are shown as means SE of 6 mice in each group. **P* 0.05. LPMC, lamina propria mononuclear cells.

etry analysis. In the colitic samples, NKG2D expression on CD4 T cells was significantly increased compared with that in normal mice (Fig. 3, *A* and *B*). Although it has been reported that murine NKG2D molecule is usually expressed on DX5 NK or NKT cells (23, 25), DX5 cells could not be detected on cells isolated from colonic tissues through conventional DTT/collagenase treatment (Fig. 3*A*). In the spleen of colitic mice, a significantly increased proportion of CD4 T cells coexpressed NKG2D, which was not observed in normal mice (Fig. 3, *A* and *B*). Interestingly, we detected DX5 cells in the spleen of both colitic and normal mice, where we found that almost all DX5 cells expressed NKG2D with high intensity (Fig. 3, *A* and *B*).

Correlation between CD4 NKG2D T cells and other costimulatory molecules. It has been recently reported that both CD4 T cells and CD8 T cells in the peripheral blood or the synovial tissue of patients with rheumatoid arthritis do not express CD28 but express NKG2D (12), indicating that NKG2D can function as a complementary molecule of other CD28 family molecules, such as CD28, ICOS, and PD-1. To address this, we assessed phenotypic correlation between these CD28 family molecules on CD4 T cells using three-color flow cytometry. Since normal splenic CD4 T cells do not express NKG2D (Fig. 3, *A* and *B*), we assessed whether three splenic populations, normal CD4 NKG2D , colitic CD4 NKG2D , colitic and CD4 NKG2D cells, express CD28, ICOS, or PD-1 on the cell surface. Unlike peripheral CD4 CD28 NKG2D cells in patients with rheumatoid arthritis (12), CD28 was expressed on colitic CD4 NKG2D to a similar extent with that on normal and colitic CD4 NKG2D cells (Fig. 4*A*). This was statistically confirmed by assessing the mean fluorescence intensity (MFI) of NKG2D expression (Fig. 4*B*, *left*). In contrast, ICOS and PD-1 molecules were markedly upregulated on colitic CD4 NKG2D and CD4 NKG2D cells but were not on normal CD4 NKG2D cells (Fig. 4, *A* and *B*). The results indicated that NKG2D expression is not associated with other representative T cell costimulatory molecules.

Expression of NKG2D ligands in the colon of CD4 CD45RB^{high} T cell-transferred SCID mice. To clarify the expression of NKG2D ligands in the colon, we next conducted quantitative real-time PCR analysis using whole colonic tissues from colitic mice or age-matched BALB/c mice. This quantitative PCR analysis revealed that mRNA expression of H60 was significantly increased in colitic colon samples compared with that in normal colon samples (Fig. 5*A*). In contrast, mRNA expression of Mult-1 and Rae-1 was not significant in colitic colon samples compared with that in normal colon samples (Fig. 5*A*). Because of the limitation of recovered cell number of immune cells from normal colon samples, we isolated IECs and LP CD4 , CD11b , and CD11c cells only from the colon of colitic mice to evaluate which NKG2D ligand is expressed in each cell population of colitic mice. As shown in Fig. 5*B*, H60 mRNA was expressed in every population, but was significantly increased in CD11c cells compared with that in other populations (Fig. 5*B*, *top*). Mult-1 mRNA was expressed exclusively in CD11c cells (Fig. 5*B*, *middle*). Rae-1 mRNA in CD11c cells was significantly increased compared with that in IECs and CD4 T cell populations, indicating that the major population expressing NKG2D ligands is CD11c dendritic cells rather than IECs in colitic mice.

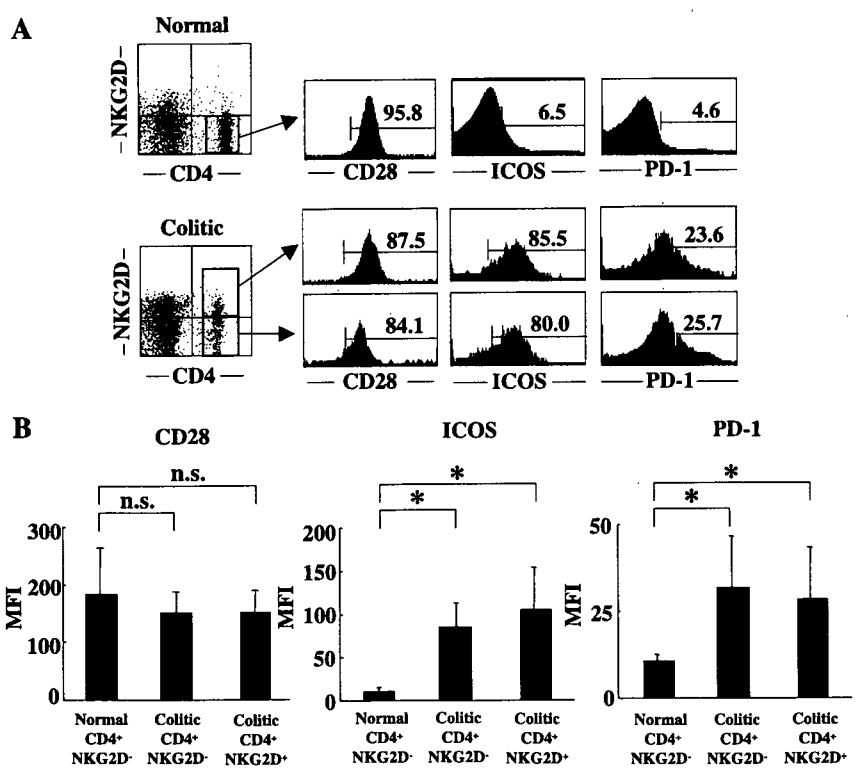

Fig. 4. Correlation between NKG2D molecule and other costimulatory molecules. *A*: expression of CD28, inducible T-cell costimulator (ICOS), and PD-1 on CD4 NKG2D and CD4 NKG2D subpopulations of splenic T cells obtained from control mice or colitic mice. Thick histograms represent staining with MAbs against the indicated markers. *B*: mean fluorescence intensity (MFI) of each costimulatory molecule on each CD4 NKG2D and CD4 NKG2D subpopulation are compared by flow cytometry. Data are shown as mean SE of 6 mice in each group. *P 0.05; n.s., not significant.

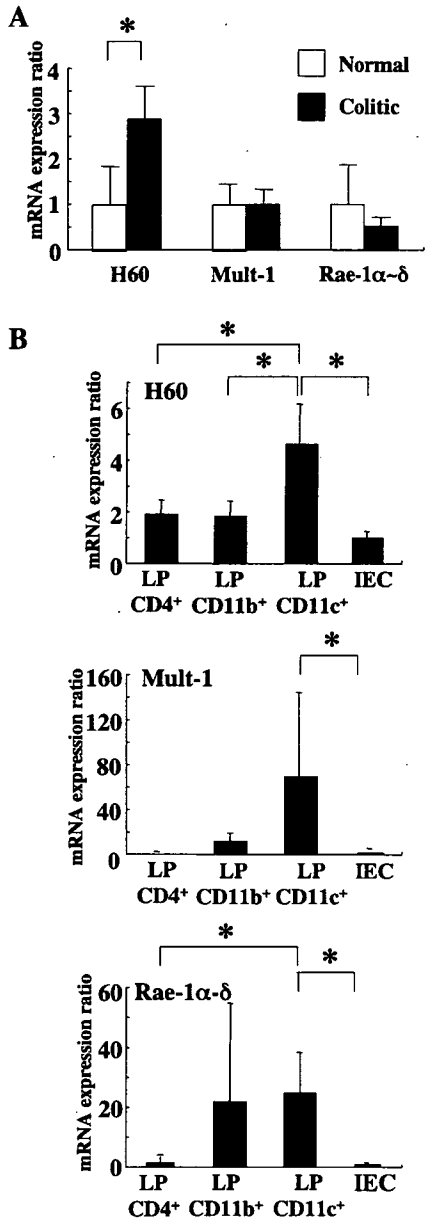

Fig. 5. Expression of H60, Mult-1, and Rae-1 mRNA in colonic samples. *A*: expression of H60, Mult-1, Rae-1, and G3PDH mRNA was determined by quantitative real-time RT-PCR using 3 whole colon samples each from normal and colitic mice. Relative mRNA expression of each ligand in colitic colon is compared with that in normal colon. Expression of H60 mRNA in colitic colon was significantly increased compared with that in normal colon. Data represent means SE of 3 independent experiments. *B*: expression of H60, Mult-1, and Rae-1 mRNA is determined by quantitative real-time RT-PCR using 3 samples each from colitic LP CD4 , CD11b , CD11c cells, and intestinal epithelial cells (IECs). Expression of H60 mRNA in colitic LP CD11c cells was significantly increased compared with other populations. Expression of Mult-1 mRNA and Rae-1 mRNA in colitic LP CD11c cells was also increased compared with that in colitic LP CD4 , CD11b cells or colitic IECs. H60 mRNA was mainly expressed in populations of CD11c cells. Data represent mean SE of 3 independent experiments.

Administration of neutralizing anti-NKG2D MAb prevents the development of colitis. The expression of NKG2D on the infiltrating LP CD4 T cells and expression of NKG2D ligands in the colitic LP suggested a possible involvement of NKG2D signaling pathway in the pathogenesis of chronic colitis. Thus, to explore the contribution of NKG2D signaling pathway in chronic colitis, nondepleting and neutralizing anti-NKG2D MAb (HMG2D) were administered to the recipient SCID mice transferred with CD4 CD45RB^{high} T cells started from the day of transfer and then three times a week for 7 wk. As shown in Fig. 6*A*, control IgG-treated mice manifested progressive weight loss (wasting disease) from 3 wk after transfer. These mice had diarrhea with increased mucus in the stool, anorectal prolapse, and hunched posture by 5–6 wk after transfer. In contrast, anti-NKG2D MAb-treated mice appeared healthy with gradual increase of body weight, and no diarrhea was observed throughout the whole period of observation (Fig. 6*A*). At 7 wk after transfer, the colon of control IgG-treated mice was enlarged and had a greatly thickened wall, which was not observed in the anti-NKG2D MAb-treated mice or mice transferred with CD4 CD45RB^{high} and CD4 CD45RB^{low} T cells (Fig. 6*B*). In addition, enlargement of the spleen and mesenteric lymph nodes were also evident in control IgG-treated mice, but not in anti-NKG2D MAb-treated mice (Fig. 6*B*). A comprehensive assessment of colitis by clinical scores showed a clear difference between control IgG-treated mice and anti-NKG2D MAb-treated mice (Fig. 6*C*).

Histological examination showed prominent epithelial hyperplasia with glandular elongation with a massive infiltration of mononuclear cells in the LP in the colon of control IgG-treated mice (Fig. 6*D*). In contrast, inflammation was mostly abrogated and only few mononuclear cells were observed in the LP of the colon from anti-NKG2D MAb-treated mice and in mice transferred with CD4 CD45RB^{high} and CD4 CD45RB^{low} T cells (Fig. 6*D*). This difference was also confirmed by histological scoring of multiple colon sections, which was 5.2 1.1 in the control rat IgG-treated mice, 2.2 0.8 in anti-NKG2D MAb-treated mice, and 1.6 0.6 in mice transferred with CD4 CD45RB^{high} and CD4 CD45RB^{low} T cells (P 0.01) (Fig. 6*E*). A further quantitative evaluation of CD4 T cell infiltration was done by isolating LP mononuclear cells from resected colons. Only a few CD4 T cells were recovered from the colonic tissue of anti-NKG2D MAb-treated mice and mice transferred with CD4 CD45RB^{high} and CD4 CD45RB^{low} T cells compared with control IgG-treated mice (Fig. 6*F*). Furthermore, the number of CD4 splenocytes from control IgG-treated mice was significantly increased compared with that from age-matched normal BALB/c mice (data not shown). In contrast, the number of CD4 splenocytes from anti-NKG2D MAb-treated mice was significantly less than that from control IgG-treated mice (data not shown).

We also examined the cytokine production by LP CD4 cells of control IgG- or anti-NKG2D MAb-treated mice. As shown in Fig. 6*G*, LP CD4 cells from anti-NKG2D MAb-treated mice produced significantly less IFN- compared with those from control IgG-treated mice upon in vitro stimulation. These results suggested that anti-NKG2D MAb prevented the development of colitis primarily by inhibiting the expansion and/or infiltration of pathogenic T cells in the colon and secondarily by inhibiting the development of pathogenic Th1 cells.

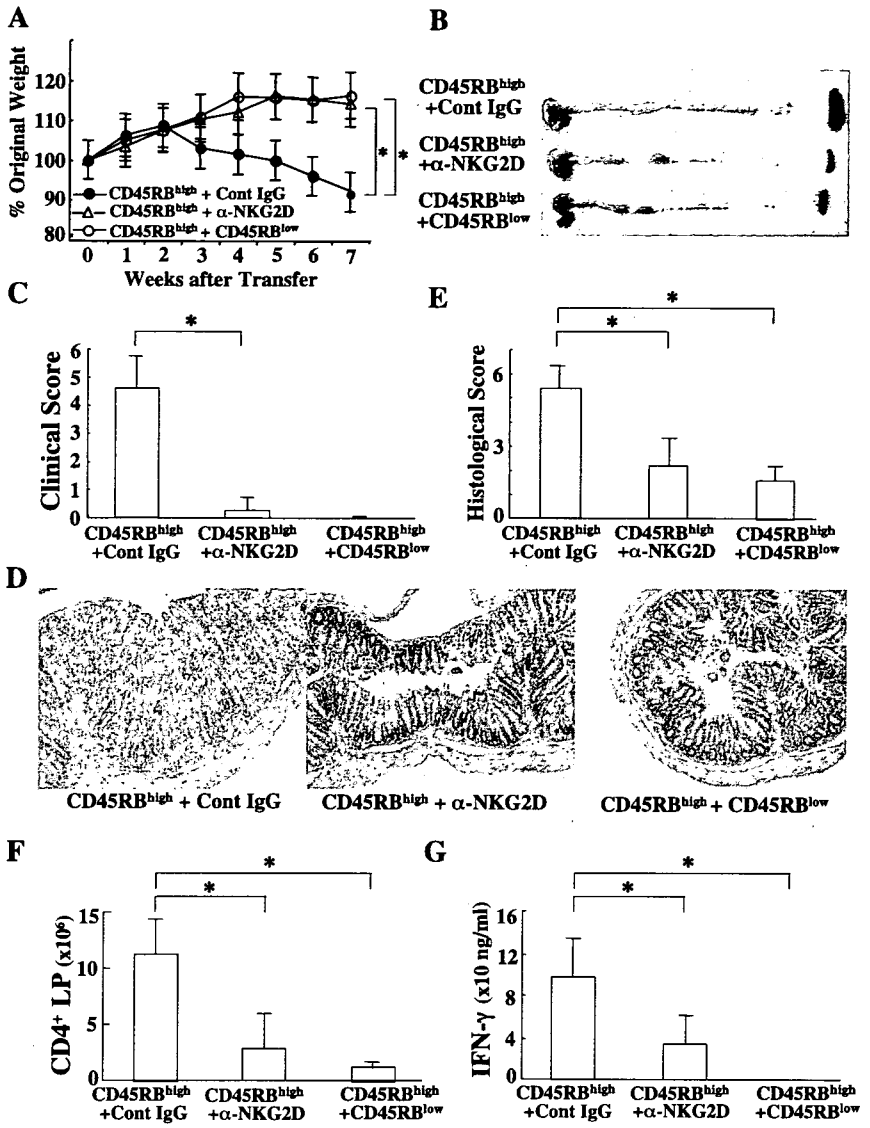

Fig. 6. Preventive effect of anti-NKG2D MAb on the development of colitis. The recipient mice were administered with anti-NKG2D MAb or control hamster IgG for 7 wk starting from the time of CD4 CD45RB^{high} T cell transfer. Other mice were transferred with CD4 CD45RB^{high} T cells and CD4 CD45RB^{low} T cells. *A*: change in body weight over time is expressed as percent of the original weight. Data represent means SE of 7 mice in each group. *P 0.05 compared with control IgG. *B*: gross appearance of the colon, mesenteric lymph nodes, and spleen 7 wk after transfer in CD4 CD45RB^{high} T cell-transferred SCID mice treated with control IgG (*top*) or anti-NKG2D MAb (*middle*), and mice transferred with CD4 CD45RB^{high} T cells and CD4 CD45RB^{low} T cells (*bottom*). *C*: clinical scores were determined at 7 wk after transfer as described in MATERIALS AND METHODS. Data indicate means SE of 7 mice in each group. *P 0.05. *D*: histological examination of the colons at 7 wk after T cell transfer. Original magnification 100. *E*: histological scoring of colitis at 7 wk after T cell transfer. Data indicate means SE of 7 mice in each group. *P 0.05. *F*: lamina propria lymphocytes (LPL) were isolated from the colon at 7 wk after transfer, and the number of CD4 cells were determined by flow cytometry. Data indicate means SE of 7 mice in each group. *P 0.01. *G*: IFN- production by LP CD4 T cells. Isolated LP CD4 T cells were stimulated with anti-CD3 and anti-CD28 MAbs for 48 h. IFN- concentration in culture supernatants were measured by mouse Th1/Th2 CBA kit. Data indicate means SE of 7 mice in each group. *P 0.05.

DISCUSSION

In the present study, we demonstrated that NKG2D signaling pathway is critically involved in the development of CD4 T cell-mediated chronic colitis by showing that LP CD4 T cells obtained from colitic SCID mice induced by adoptive transfer of CD4 CD45RB^{high} T cells express NKG2D and neutralizing anti-NKG2D MAb treatment ameliorates the development of the colitis model.

Very recently, Kjellev and colleagues (17) demonstrated that NKG2D is expressed on CD4 T cells obtained from colitic SCID mice induced by adoptive transfer of normal splenic CD4 CD25 T cells, and treatment by a neutralizing anti-NKG2D MAb (CX5) prevents the development of colitis. Their results are quite similar to ours, but it is noteworthy that normal splenic CD4 CD25 T cells that are a distinct cell population from CD4 CD25 regulatory T cells, include DX5 CD44^{high}CD45RB^{low} CD4 NKT cells along with CD44^{high} memory and CD44^{low} naive CD4 T cells (Fig. 1). Although they demonstrated that CD4 CD25 donor cells did not express NKG2D before transfer, it remained possible that NKG2D expression could be inducible on activated NKT cells rather than on activated conventional CD4 T cells especially in case of mouse models (30). In contrast, we used CD4 CD45RB^{high} T cells as donor cells, which were characterized to have a cell-surface phenotype of DX5 CD44^{low}, whereas NKT cells were DX5 CD44^{high} (Fig. 1). Thus we believe that NKG2D was solely induced on donor conventional CD4 cells after transfer in our colitis model. Interestingly, their group showed that anti-NKG2D MAb (CX5) treatment significantly decreased histological score in the colon but did not prevent the wasting disease, compared with control IgG-treated mice. In contrast, however, we here showed that our anti-NKG2D MAb (HMG2D) treatment ameliorated both the histological score and the wasting disease, although the protocol was quite similar except the phenotype of transferred donor cells (CD4 CD25 vs. CD4 CD45RB^{high}).

Notably, although the numbers of the donor cells used in these two studies were exactly the same, the kinetic of the development of colitis in control-IgG-treated SCID mice transferred with CD4 CD25 T cells in Kjellev's preventive protocol (17) was obviously more rapid (3 wk of experimental period) compared with those transferred with CD4 CD45RB^{high} T cells in our protocol (7 wk of experimental period). Although there are several explanations for the discrepancy, including differences in the status of *Helicobacter hepaticus* infection, the type of animal model, the type of blocking agents, and dosing regimens used, further studies will be needed to address this issue.

In this study, we also demonstrated using whole colonic samples by quantitative real-time RT-PCR analysis that NKG2D ligands were also expressed in colonic tissues in both colitic mice and normal mice. Expectedly, mRNA expression of H60 was significantly increased in colitic colon samples compared with that in normal colon samples, although no significant change was observed in mRNA expression of Mult-1 and Rae-1 between colitic and normal samples. This indicates a possibility that NKG2D signaling pathway modulates the development of chronic colitis and also tunes the degree of colitis.

Recent human studies have demonstrated that not only MICA, which is one of NKG2D ligands in humans, is markedly upregulated on cell surface of inflammatory IECs but also CD8 NKG2D intestinal epithelial lymphocytes (IELs) are significantly increased in patients with active celiac disease (14, 22), suggesting a possible contribution to the pathogenesis of celiac disease due to IEL-mediated damage of IECs by NKG2D-MICA interaction. Furthermore, Allez and colleagues (1) have very recently reported that MICA and NKG2D expression is significantly increased on IECs and LP CD4 T cells, respectively, in inflamed mucosa of active Crohn's disease. Although all these studies in humans focused on MICA expression in inflamed IECs, interestingly, we found that NKG2D ligands were mainly expressed in CD11c dendritic cells rather than IECs in inflamed mucosa of colitic SCID mice. Collectively, in our system, it is likely that NKG2D signaling pathway is critically involved in the interactions between T cells and APCs (especially CD11c dendritic cells) rather than IECs in intestinal mucosal immune system of chronic colitis. However, it remains unclear which ligand of NKG2D plays the dominant role in the pathogenesis of our colitic model. Further studies will be needed to address this issue.

In summary, our present findings suggest that the regulation of NKG2D signaling pathway may be of a key importance in successful treatment of chronic colitis, and targeting of NKG2D-expressing pathogenic CD4 T cells may be a useful strategy for the treatment of Th1-mediated chronic intestinal inflammation such as Crohn's disease.

GRANTS

This study was supported in part by grants-in-aid for Scientific Research, Scientific Research on Priority Areas, Exploratory Research and Creative Scientific Research from the Japanese Ministry of Education, Culture, Sports, Science and Technology; the Japanese Ministry of Health, Labor and Welfare; the Japan Medical Association; Foundation for Advancement of International Science; Ohyama Health Foundation; Yakult Bio-Science Foundation; Research Fond of Mitsukoshi Health and Welfare Foundation.

REFERENCES

1. **Allez M, Tieng V, Nakazawa A, Treton X, Pacault V, Dulphy N, Caillat-Zucman S, Paul P, Gornet JM, Duuay C, Ravet S, Tamouza R, Charron D, Lemann M, Mayer L, Toubert A.** CD4 NKG2D T cells in Crohn's disease mediate inflammatory and cytotoxic responses through MICA interactions. *Gastroenterology* 132: 2346–2358, 2007.
2. **Bamias G, Nyce MR, De La Rue SA, Cominelli F.** New concepts in the pathophysiology of inflammatory bowel disease. *Ann Intern Med* 143: 895–904, 2005.
3. **Baumgart DC, Carding SR.** Inflammatory bowel disease: cause and immunobiology. *Lancet* 369: 1627–1640, 2007.
4. **Bouma G, Strober W.** The immunological and genetic basis of inflammatory bowel disease. *Nat Rev Immunol* 3: 521–533, 2003.
5. **Carayannopoulos LN, Naidenko OV, Fremont DH, Yokoyama WM.** Cutting edge: murine UL16-binding protein-like transcript 1: a newly described transcript encoding a high-affinity ligand for murine NKG2D. *J Immunol* 169: 4079–4083, 2002.
6. **Cerwenka A, Bakker AB, McClanahan T, Wagner J, Wu J, Phillips JH, Lanier LL.** Retinoic acid early inducible genes define a ligand family for the activating NKG2D receptor in mice. *Immunity* 12: 721–727, 2000.
7. **Chambers CA.** The expanding world of co-stimulation: the two-signal model revised. *Trends Immunol* 22: 217–223, 2001.
8. **Coyle AJ, Gutierrez-Ramos JC.** The expanding B7 superfamily: increasing complexity in costimulatory signals regulating T cell function. *Nat Immunol* 2: 203–209, 2001.
9. **Diefenbach A, Jensen ER, Jamieson AM, Raulet DH.** Rae1 and H60 ligands of the NKG2D receptor stimulate tumour immunity. *Nature* 413: 165–171, 2001.
10. **Fiocchi C.** Inflammatory bowel disease: etiology and pathogenesis. *Gastroenterology* 115: 182–205, 1998.
11. **Greten FR, Eckmann L, Greten TF, Park JM, Li ZW, Egan LJ, Kagnoff MF, Karin M.** Ikk links inflammation and tumorigenesis in a mouse model of colitis-associated cancer. *Cell* 118: 285–296, 2004.
12. **Groh V, Bruhl A, El-Gabalawy H, Nelson JL, Spies T.** Stimulation of T cell autoreactivity by anomalous expression of NKG2D and its MIC ligands in rheumatoid arthritis. *Proc Natl Acad Sci USA* 100: 9452–9457, 2003.
13. **Hibi T, Ogata H.** Novel pathophysiological concepts of inflammatory bowel disease. *J Gastroenterol* 41: 10–16, 2006.
14. **Hue S, Mention JJ, Monteiro RC, Zhang S, Cellier C, Schmitz J, Verkarre V, Fodil N, Bahram S, Cerf-Bensussan N, Caillat-Zucman S.** A direct role for NKG2D/MICA interaction in villous atrophy during celiac disease. *Immunity* 21: 367–377, 2004.
15. **Jameson AM, Diefenbach A, McMahon CW, Xiong N, Carlyle JR, Raulet DH.** The role of the NKG2D immunoreceptor in immune cell activation and natural killing. *Immunity* 17: 19–29, 2002.
16. **June CH, Bluestone JA, Nadler LM, Thompson CB.** The B7 and CD28 receptor families. *Immunology Today* 15: 321–331, 1994.
17. **Kjellev S, Haase C, Lundsgaard D, Urso B, Tornehave D, Markholst H.** Inhibition of NKG2D receptor function by antibody therapy attenuates transfer-induced colitis in SCID mice. *Eur J Immunol* 37: 1397–1406, 2007.
18. **Liu Z, Geboes K, Colpaert S, Overbergh L, Mathieu C, Heremans H, de Boer M, Boon L, D'Haens G, Rutgeerts P, Ceuppens JL.** Prevention of experimental colitis in SCID mice reconstituted with CD45RB^{high}CD4 T cells by blocking the CD40-CD154 interactions. *J Immunol* 164: 6005–6014, 2000.
19. **Makita S, Kanai T, Nemoto Y, Totsuka T, Okamoto R, Tsuchiya K, Yamamoto M, Kiyono H, Watanabe M.** Intestinal lamina propria retaining CD4 CD25 regulatory T cells is a suppressive site of intestinal inflammation. *J Immunol* 178: 4937–4946, 2007.
20. **Malarkannan S, Shih PP, Eden PA, Horng T, Zuberi AR, Christianson G, Roopenian D, Shastri N.** The molecular and functional characterization of a dominant minor H antigen, H60. *J Immunol* 161: 3501–3509, 1998.
21. **Malmstrom V, Shipton D, Singh B, Al-Shamkhani A, Puklavec MJ, Barclay AN, Powrie F.** CD134L expression on dendritic cells in the mesenteric lymph nodes drives colitis in T cell-restored SCID mice. *J Immunol* 166: 6972–6981, 2001.
22. **Meresse B, Chen Z, Ciszewski C, Tretiakova M, Bhagat G, Krausz TN, Raulet DH, Lanier LL, Groh V, Spies T, Ebert EC, Green PH, Jabri B.** Coordinated induction by IL15 of a TCR-independent NKG2D signaling pathway converts CTL into lyphokine-activated killer cells in celiac disease. *Immunity* 21: 357–366, 2004.

23. **Ogasawara K, Lanier LL.** NKG2D in NK and T cell-mediated immunity. *J Clin Immunol* 25: 534–540, 2005.
24. **Podolsky DK.** Inflammatory bowel disease. *N Engl J Med* 347: 417–429, 2002.
25. **Raulet DH.** Roles of the NKG2D immunoreceptor and its ligands. *Nat Rev Immunol* 3: 781–790, 2003.
26. **Sandborn WJ, Targan SR.** Biologic therapy of inflammatory bowel disease. *Gastroenterology* 122: 1592–1608, 2002.
27. **Totsuka T, Kanai T, Iiyama R, Uraushihara K, Yamazaki M, Okamoto R, Hibi T, Tezuka K, Azuma M, Akiba H, Yagita H, Okumura K, Watanabe M.** Ameliorating effect of anti-ICOS monoclonal antibody in a murine model of chronic colitis. *Gastroenterology* 124: 410–421, 2003.
28. **Totsuka T, Kanai T, Makita S, Fujii R, Nemoto Y, Oshima S, Okamoto R, Koyanagi A, Akiba H, Okumura K, Yagita H, Watanabe M.** Regulation of murine chronic colitis by CD4 CD25 programmed death-1 T cells. *Eur J Immunol* 35: 1773–1785, 2005.
29. **Uraushihara K, Kanai T, Ko K, Totsuka T, Makita S, Iiyama R, Nakamura T, Watanabe M.** Regulation of murine inflammatory bowel disease by CD25 and CD25 CD4 glucocorticoid-induced TNF receptor family-related gene regulatory T cells. *J Immunol* 171: 708–716, 2003.
30. **Yoshimoto T, Paul WE.** CD4 NK1.1 T cells promptly produce interleukin 4 in response to in vivo challenge with anti-CD3. *J Exp Med* 179: 1285–1295, 1994.

IL-7 Is Essential for the Development and the Persistence of Chronic Colitis[1]

Teruji Totsuka, Takanori Kanai,[2] Yasuhiro Nemoto, Shin Makita, Ryuichi Okamoto, Kiichiro Tsuchiya, and Mamoru Watanabe

Although IL-7 has recently emerged as a key cytokine involved in controlling the homeostatic turnover and the survival of peripheral resting memory CD4 T cells, its potential to be sustained pathogenic CD4 T cells in chronic immune diseases, such as inflammatory bowel diseases, still remains unclear. In this study, we demonstrate that IL-7 is essential for the development and the persistence of chronic colitis induced by adoptive transfer of normal CD4 CD45RB^{high} T cells or colitogenic lamina propria (LP) CD4 memory T cells into immunodeficient IL-7 / RAG-1 / and IL-7 / RAG-1 / mice. Although IL-7 / RAG-1 / recipients transferred with CD4 CD45RB^{high} splenocytes developed massive inflammation of the large intestinal mucosa concurrent with massive expansion of Th1 cells, IL-7 / RAG-1 / recipients did not. Furthermore, IL-7 / RAG-1 /, but not IL-7 / RAG-1 /, mice transferred with LP CD4 CD44^{high}CD62L IL-7R ^{high} effector-memory T cells (T_{EM}) isolated from colitic CD4 CD45RB^{high}-transferred mice did not develop colitis. Although rapid proliferation of transferred colitogenic LP CD4 T_{EM} cells was observed in the in IL-7 / RAG-1 / mice to a similar extent of those in IL-7 / RAG-1 / mice, Bcl-2 expression was significantly down-modulated in the transferred CD4 T cells in IL-7 / RAG-1 / mice compared with those in IL-7 / RAG-1 / mice. Taken together, IL-7 is essential for the development and the persistence of chronic colitis as a critical survival factor for colitogenic CD4 T_{EM} cells, suggesting that therapeutic approaches targeting IL-7/IL-7R signaling pathway may be feasible in the treatment of inflammatory bowel diseases. *The Journal of Immunology,* **2007, 178: 4737–4748.**

Inflammatory bowel diseases (IBD)[3] is caused by excessive and tissue damaging chronic inflammatory responses in the gut wall and commonly take persistent, disabling courses (1). In some patients, disease progresses steadily, while in others, relapses alter with remissions. According to present understanding, disease is caused and controlled by pathogenic effector and memory CD4 T cells, which are accumulated in their target tissues and thus determine activity and clinical character. However, the nature of pathogenic memory CD4 T cells over time and the correlation between effector and memory CD4 T cells in chronic colitis in the presence of commensal bacteria remains largely unknown.

IL-7 is a stromal cell-derived cytokine that is secreted by fetal liver cells, stromal cells in the bone marrow and thymus, and other epithelial cells (2–4). Recently, IL-7 has emerged as a key cytokine involved in controlling the survival of peripheral resting CD4 T cells, including naive and memory cells and their homeostatic turnover (3–10). The effect of IL-7 on T cells is controlled by the expression of the specific receptor for IL-7, the state of differentiation of the T cell, the available concentration of the cytokine, and whether there is concomitant TCR signaling. IL-7R consists of the -chain (CD127) and the common cytokine receptor -chain, which is shared by the common -chain family cytokines (IL-2, IL-4, IL-9, IL-15, and IL-21) (3, 4).

In contrast to the role of IL-7 in naive and memory CD4 T cells in the resting state, the pathological role of IL-7 in chronic immune-mediated diseases, such as autoimmune diseases and IBD, remains largely unclear. We have previously demonstrated that 1) IL-7 is constitutively produced by intestinal epithelial cells (11), 2) IL-7 transgenic mice developed chronic colitis that mimicked histopathological characteristics of human IBD (12), 3) mucosal CD4 IL-7R^{high} T cells in mice with colitis are colitogenic (13), and 4) the selective elimination of CD4 IL-7R^{high} T cells by administrating small amounts of toxin-conjugated anti-IL-7R mAb completely ameliorated ongoing colitis (13).

In this study, we attempt to clarify the link between the colitogenic CD4 T cells and IL-7 more extensively in terms of pathogenesis of chronic colitis using adoptive transfer system. The adoptive transfer of CD4 CD45RB^{high} T cells into syngeneic immunodeficient mice, such as SCID mice and RAG-1 or RAG-2-deficient mice, induces human IBD-like diseases (14). The key factors for the development of colitis are an expanding CD4 T cell subset in lymphopenic condition, an intact gut flora of the host, and various cytokines (15). Dysregulation of mucosal CD4 T cell responses is supposed to play a key role in the pathogenesis of colitis in this model, with exaggerated IFN- and TNF- responses as major mediators of these models (14, 15). These pathogenic CD4 T cell responses may be derived by Ags of the intestinal flora to which these CD4 T cells are normally tolerant in the presence of regulatory T cells. Because the use of IL-7 / or IL-7R / mice in inflammatory models is not useful because of the

Department of Gastroenterology and Hepatology, Graduate School, Tokyo Medical and Dental University, Tokyo, Japan

Received for publication May 15, 2006. Accepted for publication January 8, 2007.

The costs of publication of this article were defrayed in part by the payment of page charges. This article must therefore be hereby marked *advertisement* in accordance with 18 U.S.C. Section 1734 solely to indicate this fact.

[1] This study was supported in part by grants-in-aid for Scientific Research, Scientific Research on Priority Areas, Exploratory Research, and Creative Scientific Research from the Japanese Ministry of Education, Culture, Sports, Science and Technology; the Japanese Ministry of Health, Labor and Welfare; the Japan Medical Association; Foundation for Advancement of International Science; Terumo Life Science Foundation; Ohyama Health Foundation; Yakult Bio-Science Foundation; and Research Fond of Mitsukoshi Health and Welfare Foundation.

[2] Address correspondence and reprint requests to Dr. Takanori Kanai, Department of Gastroenterology and Hepatology, Tokyo Medical and Dental University, 1-5-45 Yushima, Bunkyo-ku, Tokyo, Japan. E-mail address: taka.gast@tmd.ac.jp

[3] Abbreviations used in this paper: IBD, inflammatory bowel disease; HPF, high power field; IEL, intraepithelial cell; LP, lamina propria; T_{EM}, effector-memory T.

Copyright © 2007 by The American Association of Immunologists, Inc. 0022-1767/07/$2.00

lymphoid organ aberrations and the lack of lymphocytes (3), we, in this study, used IL-7 ′ RAG-1 ′ and IL-7 ′ RAG-1 ′ mice for adoptive transfer of CD4 CD45RB^{high} T cells and colitogenic lamina propria (LP) CD4 CD44^{high}CD62L IL-7R ^{high} effector-memory T (T_{EM}) cells obtained from colitic mice that have been transferred previously with CD4 CD45RB^{high} T cells to assess a role of IL-7 for the development and the persistence of chronic colitis. We studied this polyclonal system rather than system using monoclonal TCR transgenic memory CD4 T cells because they not only represent a diverse memory pool, but they also provide the most pathophysiolocally relevant setting to examine the role of IL-7 in the development of colitis.

Materials and Methods

Animals

Female C57BL/6 mice were purchased from Japan CLEA. C57BL/6 background RAG-2 ′ mice were obtained from Taconic Farms. C57BL/6 background RAG-1 ′ mice and C57BL/6 background IL-7-deficient (IL-7 ′) mice were provided from Dr. R. Zamoyska (National Institute for Medical Research, London, U.K.) (16). IL-7 ′ mice were intercrossed into RAG-1 ′ mice to generate IL-7 ′ RAG-1 ′ mice in the Animal Care Facility of Tokyo Medical and Dental University. Mice were maintained under specific pathogen-free conditions in the Animal Care Facility of Tokyo Medical and Dental University. Female donors and recipients were used at 6–12 wk of age. All experiments were approved by the regional animal study committees and were done according to institutional guidelines and Home Office regulations.

Purification of T cell subsets

CD4 T cells were isolated from spleen cells from C57BL/6 mice using the anti-CD4 (L3T4)-MACS system (Miltenyi Biotec) according to the manufacturer's instruction. Enriched CD4 T cells (96–97% pure, as estimated by FACSCalibur (BD Biosciences)) were then labeled with PE-conjugated anti-mouse CD4 (RM4-5; BD Pharmingen) and FITC-conjugated anti-CD45RB (16A; BD Pharmingen). Subpopulations of CD4 cells were generated by two-color sorting on a FACSVantage (BD Biosciences). All populations were 98.0% pure on reanalysis. To isolate LP CD4 T cells, colitis was induced in RAG-2 ′ mice by adoptive transfer of CD4 CD45RB^{high} T cells as described previously (17). The colitic CD4 CD45RB^{high} T cell-transferred RAG-2 ′ mice were sacrificed at 6–8 wk after transfer. The entire length of colon was opened longitudinally, washed with PBS, and cut into small pieces. The dissected mucosa was incubated with Ca^2 -, Mg^2 -free Hanks' BSS containing 1 mM DTT (Sigma-Aldrich) for 45 min to remove mucus and then treated with 2.0 mg/ml collagenase (Worthington Biomedical) and 0.01% DNase (Worthington Biomedical) for 2 h. The cells were pelleted two times through a 40% isotonic Percoll solution and then subjected to Ficoll-Hypaque density gradient centrifugation (40/75%). Enriched LP CD4 T cells were obtained by positive selection using anti-CD4 (L3T4) MACS magnetic beads. The resultant cells when analyzed by FACSCalibur contained 95% CD4 cells.

In vivo experimental design

We performed a series of in vivo experiments below to investigate the role of IL-7 in the development and the persistence of murine chronic colitis. Experiment 1: To assess the necessity of IL-7 in the initial development of colitis, including the processes for T cell priming, activation, and persistence of pathogenic effector and memory CD4 T cells, we performed the cell transfer experiments using IL-7 ′ RAG-1 ′ and IL-7 ′ RAG-1 ′ littermate recipients. IL-7 ′ RAG-1 ′ mice (n 10) and IL-7 ′ RAG-1 ′ mice (n 10) were injected i.p. with 3 10^5 splenic CD4 CD45RB^{high} T cells from normal C57BL/6 mice. Experiment 2: To assess the necessity of IL-7 for the persistence of colitogenic memory CD4 T cells, we performed the adoptive retransfer of colitogenic LP memory CD4 T cells. First, colitis was induced in RAG-2 ′ mice by adoptive transfer of CD4 CD45RB^{high} T cells. The colitogenic memory CD4 LP T cells were obtained from the colitic mice induced by adoptive transfer of CD4 CD45RB^{high} T cells 6–8 wk after transfer and then were injected again into the control IL-7 ′ RAG-1 ′ mice (IL-7 ′ 3 IL-7 ′ ; n 10) and IL-7 ′ RAG-1 ′ mice (IL-7 ′ 3 IL-7 ′ ; n 10). Experiment 3: To assess the initial role of IL-7 for T cell priming, differentiation, and sustainment of colitogenic effector and memory CD4 T cells, we performed another adoptive retransfer experiment. First, IL-7 ′ RAG-1 ′ mice were transferred with CD4 CD45RB^{high} T cells. Six weeks after transfer, splenic CD4 T cells were isolated from the transferred IL-7 ′ RAG-1 ′ mice and retransferred into new IL-7 ′ RAG-1 ′ mice (IL-7 ′ 3 IL-7 ′ ; n 7). As a positive control, splenic CD4 T cells obtained from colitic IL-7 ′ RAG-1 ′ mice that have been initially transferred with CD4 CD45RB^{high} T cells were also transferred into new IL-7 ′ RAG-1 ′ mice (IL-7 ′ 3 IL-7 ′ ; n 7). The recipient mice after transfer were weighed initially and then three times per week. They were also observed for clinical signs such as hunched posture, piloerection, diarrhea, and blood in the stool. Mice were sacrificed 4–8 wk after transfer and assessed for a clinical score (17) that is the sum of three parameters as follows: hunching and wasting, 0 or 1; colon thickening, 0–3 (0, no colon thickening; 1, mild thickening; 2, moderate thickening; 3, extensive thickening); and stool consistency, 0–3 (0, normal beaded stool; 1, soft stool; 2, diarrhea; 3, bloody stool) (17).

Histological examination

Tissue samples were fixed in PBS containing 6% neutral-buffered formalin. Paraffin-embedded sections (5 m) were stained with H&E. Three tissue samples from the proximal, middle, and distal parts of the colon were prepared. The sections were analyzed without prior knowledge of the type of T cell reconstitution or treatment. The area most affected was graded by the number and severity of lesions. The mean degree of inflammation in the colon was calculated using a modification of a previously described scoring system (17), as follows: mucosa damage, 0; normal, 1; 3–10 intraepithelial cells (IEL)/high power field (HPF) and focal damage, 2; 10 IEL/HPF and rare crypt abscesses, 3; 10 IEL/HPF, multiple crypt abscesses and erosion/ulceration, submucosa damage, 0; normal or widely scattered leukocytes, 1; focal aggregates of leukocytes, 2; diffuse leukocyte infiltration with expansion of submucosa, 3; diffuse leukocyte infiltration, muscularis damage, 0; normal or widely scattered leukocytes, 1; widely scattered leukocyte aggregates between muscle layers, 2; leukocyte infiltration with focal effacement of the muscularis, 3; extensive leukocyte infiltration with transmural effacement of the muscularis.

Cytokine ELISA

To measure cytokine production, 1 10^5 LP CD4 T cells were cultured in 200 l of culture medium at 37°C in a humidified atmosphere containing 5% CO_2 in 96-well plates (Costar) precoated with 5 g/ml hamster anti-mouse CD3 mAb (145-2C11; BD Pharmingen) and hamster 2 g/ml anti-mouse CD28 mAb (37.51; BD Pharmingen) in PBS overnight at 4°C. Culture supernatants were removed after 48 h and assayed for cytokine production. Cytokine concentrations were determined by specific ELISA per manufacturer's recommendation (R&D Systems).

Flow cytometry

To detect the surface expression of a variety of molecules, isolated splenocytes or LP mononuclear cells were preincubated with a Fc R-blocking mAb (CD16/32, 2.4G2; BD Pharmingen) for 20 min followed by incubation with specific FITC-, PE-, PECy5-, or biotin-labeled Abs for 30 min on ice. The following mAbs other than biotin-conjugated anti-mouse IL-7R (A7R34; Immuno-Biological Laboratories) were obtained from BD Pharmingen: anti-CD4 mAb (RM4-5), anti-CD25 mAb (7D4), anti-CD45RB mAb (16A), anti-CD62L mAb (MEL-14), anti-CD44 mAb (IM7), anti-CD69 mAb (H1.2F3), and anti-Bcl-2 mAb (3F11). Biotinylated Abs were detected with PE- or CyChrome-streptavidin. Standard two- or three- color flow cytometric analyses were obtained using the FACSCalibur using CellQuest software. Background fluorescence was assessed by staining with control irrelevant isotype-matched mAbs.

To analyze Bcl-2 expression in LP CD4 T cells, cells were fixed and permeabilized with BD Cytofix/Cytoperm solution before intracellular cytokine staining with FITC-conjugated anti-Bcl-2 mAb (BD Pharmingen). To analyze the TCR V family repertoire, splenic cells were double-stained with PE-conjugated anti-CD4 mAb (RM4-5), and the following FITC-conjugated mAbs: V 2; KJ25, V 3; KT4, V 4; MR9-4, V 5; RR4-7, V 6; TR310, V 7; MR5-2, V 8.1/2; B21.14, V 8.3; MR10-2, V 9; B21.5, V 10; RR3-15, V 11; MR11-1, V 12; IN12.3, V 13; 14.2, V 14; and KJ23, V 17. All Abs were purchased from BD Pharmingen.

CFSE labeling of T cells

T cell division in vivo was assessed by flow cytometry of CFSE-labeled cells. Isolated LP CD4 T cells were stained in vitro with the cytoplasmic dye CFSE (Molecular Probes) before reconstitution. Briefly, cells were incubated for 7 min at 37°C with 5 M CFSE. The reaction was quenched by washing in ice-cold DMEM supplemented with 10% FCS. The recipient mice were injected i.p. with 3.0 10^6 CFSE-labeled CD4 T cells for

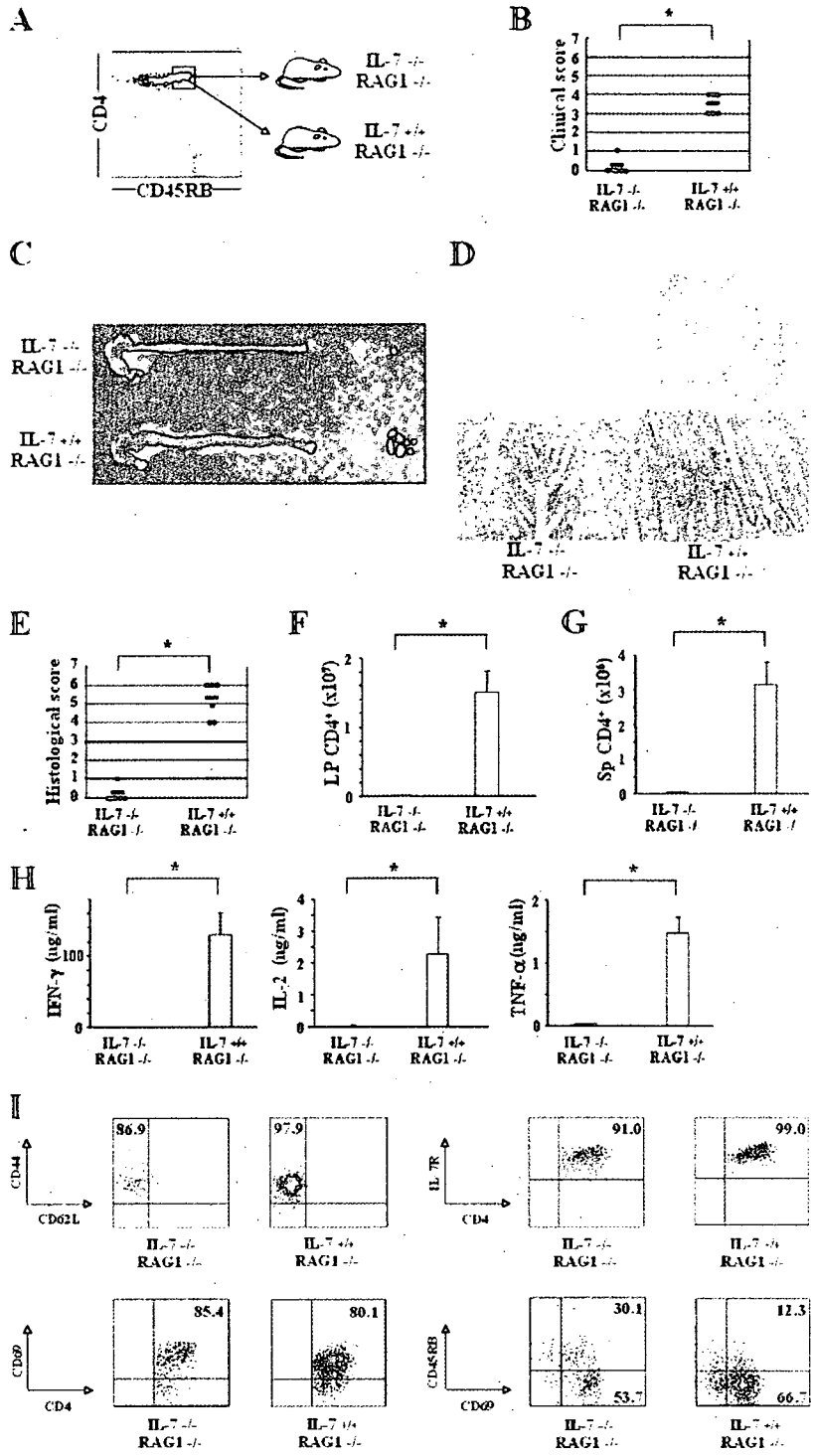

FIGURE 1. IL-7 / RAG-1 / transferred with CD4 CD45RB^{high} T cells did not develop chronic colitis. *A*, IL-7 / RAG-1 / (*n* 10) and IL-7 / RAG-1 / (*n* 10) mice were transferred with normal splenic CD4 CD45RB^{high} T cells (3 10^5 cells/mouse). *B*, Clinical scores were determined at 8 wk after the transfer as described in *Materials and Methods*. Data are indicated as the mean SEM of seven mice in each group. , p 0.001. *C*, Gross appearance of the colon, spleen, and mesenteric lymph nodes from CD4 CD45RB^{high} T cell-transferred IL-7 / RAG-1 / (*top*) and IL-7 / RAG-1 / (*bottom*) mice at 8 wk after the transfer. *D*, Histological examination of the colon from IL-7 / RAG-1 / and IL-7 / RAG-1 / recipients at 6 wk after the transfer. Original magnification: 40 (*upper*); 100 (*lower*). *E*, Histological scoring of IL-7 / RAG-1 / and IL-7 / RAG-1 / mice transferred with CD4 CD45RB^{high} T cells after 8 wk after transfer. Data are indicated as the mean SEM of seven mice in each group. , p 0.005. LP (*F*) and spleen (*G*) CD4 T cells were isolated from IL-7 / RAG-1 / and IL-7 / RAG-1 / mice transferred with CD4 CD45RB^{high} T cells 8 wk after transfer, and the number of CD4 cells was determined by flow cytometry. Data are indicated as the mean SEM of seven mice in each group. , p 0.01. *H*, Cytokine production by LP CD4 T cells. LP CD4 T cells were isolated at 8 wk after transfer and stimulated with anti-CD3 and anti-CD28 mAbs for 48 h. IFN- , IL-2, and TNF- concentrations in culture supernatants were measured by ELISA. Data are indicated as the mean SD of seven mice in each group. , p 0.001. *I*, Phenotypic characterization of LP CD4 T cells isolated from IL-7 / RAG-1 / and IL-7 / RAG-1 / mice transferred with CD4 CD45RB^{high} T cells 8 wk after transfer.

5–10 days. At the indicated time points, isolated splenic cells were stained with allophycocyanin-labeled anti-CD4 mAb (L3T4), PerCP-labeled anti-CD3 mAb (2C11), and PE-labeled Annexin V (MBL), and the intensity of CFSE and annexin V was determined after gating on CD3 CD4 T cells. To assess the role of commensal bacteria in cell division, a group of mice were treated with a set of four antibiotics, i.e., ampicillin (1g/L; Sigma-Aldrich), vancomycin (500 mg/L; Abbott Laboratories), neomycin sulfate (1 g/L; Pharmacia), and metronidazole (1 g/L; Sidmack) in drinking water 2 wk before beginning the adoptive transfer and during the course of experiment based on a variation of the commensal depletion protocol of Fagarasan et al. (18). At the indicated time points, isolated spleen cells were stained with APC-labeled anti-CD4 mAb and PerCP-labeled anti-CD3 mAb, and the intensity of CFSE was determined after gating on CD3 CD4 T cells.

Statistical analysis

The results were expressed as the mean SD. Groups of data were compared by Mann-Whitney *U* test. Differences were considered to be statistically significant when p 0.05.

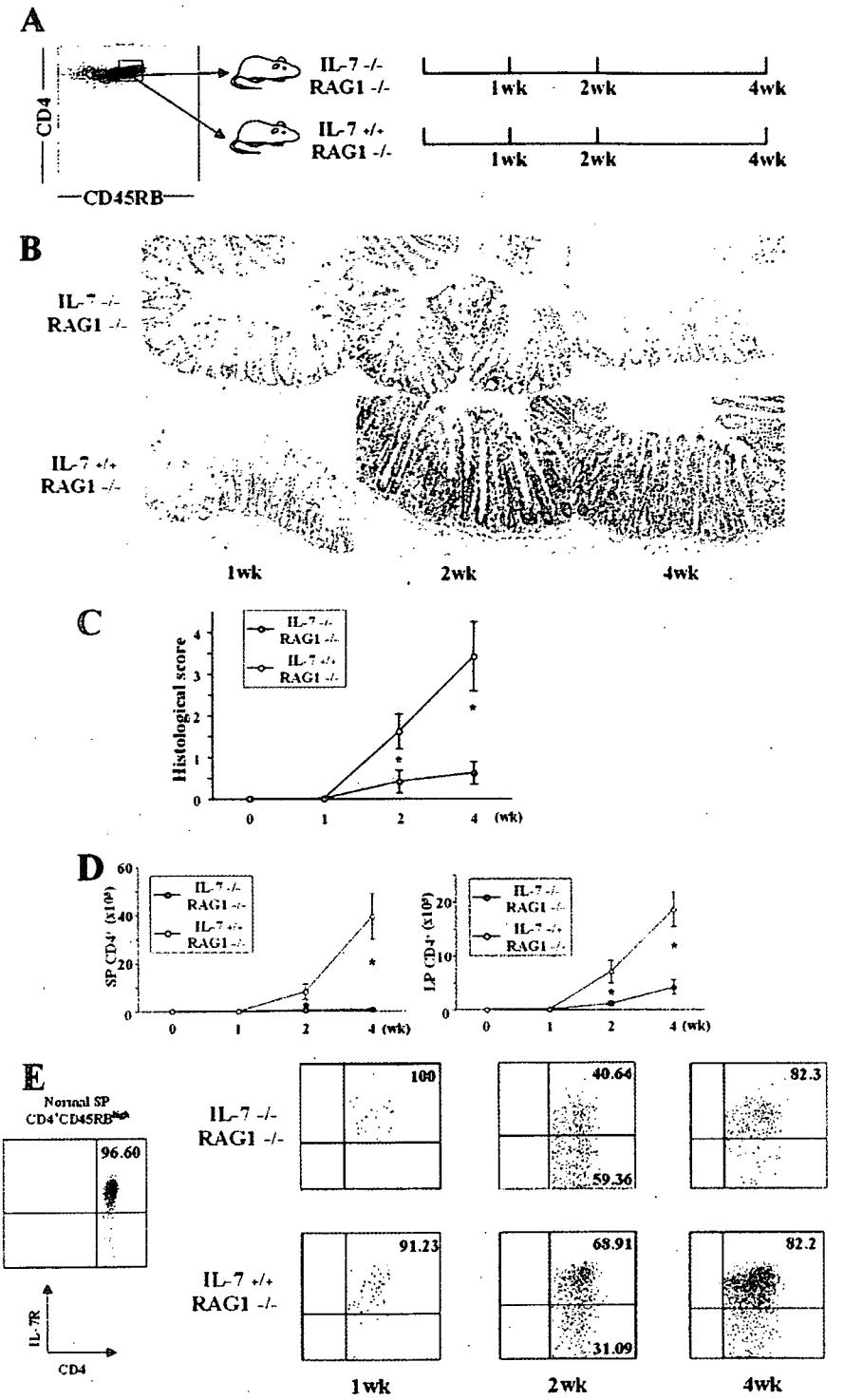

FIGURE 2. Kinetics of development of colitis and IL-7R expression. *A*, IL-7 / RAG-1 / (*n* 12) and IL-7 / RAG-1 / (*n* 10) mice were transferred with CD4 CD45RB^{high} T cells (3 10^5 cells/mouse) and assessed at the indicated time points (each *n* 4). *B*, Histological examination of the colon from IL-7 / RAG-1 / and IL-7 / RAG-1 / mice transferred with colitogenic LP CD4 CD44^{high}CD62L T_{EM} cells at 1, 2, and 4 wk after transfer. Colonic sections were stained with H&E and photographed at 100 magnification. *C*, Histological scoring of IL-7 / RAG-1 / and IL-7 / RAG-1 / recipients at the indicated time points. Data are indicated as the mean SEM of seven mice in each group. , p 0.05. *D*, Cell number of splenic and LP CD4 T cells recovered from IL-7 / Rag-1 / and IL-7 / Rag-1 / recipients. Data are indicated as the mean SEM of seven mice in each group. , p 0.05. *E*, Cell surface IL-7R expression on CD4 CD45RB^{high} T cells before transfer and LP CD4 T cells from IL-7 / Rag-1 / and IL-7 / Rag-1 / recipients at the indicated time points.

Results

Lack of colitis in IL-7 / RAG-1 / mice transferred with CD4 CD45RB^{high} T cells

We used a chronic colitis model induced by an adoptive transfer of splenic CD4 CD45RB^{high} T cells from normal C57BL/6 mice into IL-7 / RAG-1 / and IL-7 / RAG-1 / littermate recipients to assess a requirement of IL-7 for the development of chronic colitis (Fig. 1*A*). Consistent with previous reports (14), the control IL-7 / RAG-1 / mice manifested progressive weight loss from 3 wk after transfer (data not shown) and clinical symptoms of colitis as shown as clinical scores estimated by diarrhea with increased mucus in the stool, anorectal prolapse, hunched posture, and weight loss by 8 wk after transfer (Fig. 1*B*). In contrast, the IL-7 / RAG-1 / mice transferred with

CD4 CD45RB^{high} T cells showed no clinical signs of colitis and weight loss throughout the entire observation periods (Fig. 1*B*). At 8 wk after transfer, the colon from the transferred IL-7 / RAG-1 / mice, but not that from the transferred IL-7 / RAG-1 / mice, was enlarged and had a greatly thickened wall (Fig. 1*C*). In addition, the enlargement of the spleen and mesenteric lymph nodes was also present in the control IL-7 / RAG-1 / mice transferred with CD4 CD45RB^{high} T cells as compared with the IL-7 / RAG-1 / mice transferred with CD4 CD45RB^{high} T cells (Fig. 1*C*). Totally, the assessment of colitis by clinical scores showed a clear difference between the transferred IL-7 / RAG-1 / mice and the transferred IL-7 / RAG-1 / mice (Fig. 1*B*). Histological examination showed prominent epithelial hyperplasia with glandular elongation with a massive infiltration of mononuclear cells in the LP of the colon from the transferred IL-7 / RAG-1 / mice (Fig. 1*D*). In contrast, the glandular elongation was mostly abrogated, and only a few mononuclear cells were observed in the LP of the colon from the transferred IL-7 / RAG-1 / mice (Fig. 1*D*). This difference was also confirmed by histological scoring of multiple colon sections, which was 0.16 0.04 in the transferred IL-7 / RAG-1 / mice vs 5.16 0.19 in the transferred IL-7 / RAG-1 / mice (p 0.01) (Fig. 1*E*). We confirmed that the IL-7 / RAG-1 / mice transferred with CD4 CD45RB^{high} T cells did not develop intestinal inflammation cells until 20 wk of observation after transfer (data not shown).

A further quantitative evaluation of CD4 T cell infiltration was made by isolating LP and splenic CD4 T cells. Only a few CD4 T cells were recovered from the colonic tissue of the transferred IL-7 / RAG-1 / mice as compared with the transferred IL-7 / RAG-1 / mice (Fig. 1*F*). The number of CD4 cells recovered from the colon of the transferred IL-7 / RAG-1 / mice (150.5 3.23 10^5) far exceeded the number of originally injected cells (3.0 10^5), indicating an extensive T cell proliferation and survival in the inflamed colon, which was mostly abrogated in the transferred IL-7 / RAG-1 / mice (0.60 0.65 10^5) (Fig. 1*F*). Furthermore, the number of CD4 splenocytes from the transferred IL-7 / RAG-1 / mice was also significantly increased as comparable to that from the transferred IL-7 / RAG-1 / recipients (Fig. 1*G*). We also examined the cytokine production by LP CD4 T cells from the transferred IL-7 / RAG-1 / mice and the transferred IL-7 / Rag-1 / mice. As shown in Fig. 1*H*, LP CD4 T cells from the transferred IL-7 / RAG-1 / mice produced significantly less IFN- , IL-2, and TNF- as compared with those from the transferred IL-7 / RAG-1 / mice upon in vitro stimulation. Importantly, flow cytometry analysis revealed that the LP CD4 T cells isolated from both IL-7 / RAG-1 / and IL-7 / RAG-1 / recipients 8 wk after an adoptive transfer of CD4 CD45RB^{high} T cells were CD44^{high}CD62L CD69 CD45RB^{low}IL-7R ^{high} (Fig. 1*I*), indicating that the transferred CD4 CD45RB^{high} T cells could differentiate to activated T_{EM} cells even in the absence of IL-7. These results suggest that the lack of IL-7 prevented the development of colitis primarily by inhibiting the expansion and/or survival of colitigenic CD4 T_{EM} cells in the colon and secondarily by inhibiting the development of the Th1 T_{EM} cells.

Kinetics of development of colitis and IL-7R expression

When the immune system is first challenged by exposure to Ags, naive CD4 T cells become activated and undergo many rounds of expansion as they differentiate into effector and memory CD4 T cells. Because it is believed that IL-7 is not involved in the initial expansion of the effector cells but its role in maintaining pool size may influence either the onset or maintenance of colitis, we assessed the kinetics of the development of colitis and IL-7R expression to determine whether IL-7 is crucial for the onset of colitis in our model (Fig. 2*A*). At 1 wk after an adoptive transfer of CD4 CD45RB^{high} T cells into IL-7 / RAG-1 / and IL-7 / RAG-1 / mice, both mice did not develop colitis (Fig. 2*B*), and the average histological scores in both mice were 0 (Fig. 2*C*). At 2 wk after the transfer, however, the transferred IL-7 / RAG-1 / recipients develop mild colitis, characterized with the infiltration of a small number of mononuclear cells in the LP, but the transferred IL-7 / RAG-1 / recipients did not (Fig. 2*B*). The average histology scores revealed that the transferred IL-7 / RAG-1 / recipients had significantly higher colitis scores as compared with the transferred IL-7 / RAG-1 / recipients (Fig. 2*C*). Four weeks after the transfer, the difference between two groups was more apparent, as the transferred IL-7 / RAG-1 / mice developed more severe colitis, but the transferred IL-7 / RAG-1 / mice did not (Fig. 2, *B* and *C*). To examine the effects of IL-7 on the expansion of CD4 T cells in the recipients, we compared the infiltration of CD4 T cells by determining the number of CD4 T cells in the spleen and the LP by FACS analysis. In accordance with the histological scores, the average number of LP and splenic CD4 T cells recovered from the transferred IL-7 / RAG-1 / recipients were significantly increased from 2 wk after the transfer as compared with those from the transferred IL-7 / RAG-1 / recipients (Fig. 2*D*).

To obtain a more comprehensive understanding of the development of effector and memory CD4 T cells over time in this setting, we carefully examined the cell surface expression of IL-7R on LP CD4 T cells obtained from the recipients at the indicated time points. As shown in Fig. 2*E*, the splenic CD4 T cells (donor CD4 CD45RB^{high} T cells) before the transfer (0 wk) and the LP CD4 T cells after 1 wk of transfer highly expressed IL-7R , but approximately half of CD4 T cells from both the transferred IL-7 / RAG-1 / and IL-7 / RAG-1 / recipients had down-regulated IL-7R at 2 wk after transfer. However, a large portion of LP CD4 T cells from both the transferred mice at 4 wk after the transfer had regained higher expression of IL-7R to 80% per total CD4 T cells (Fig. 2*E*). These data indicate that IL-7R expression was regulated during T cell differentiation from

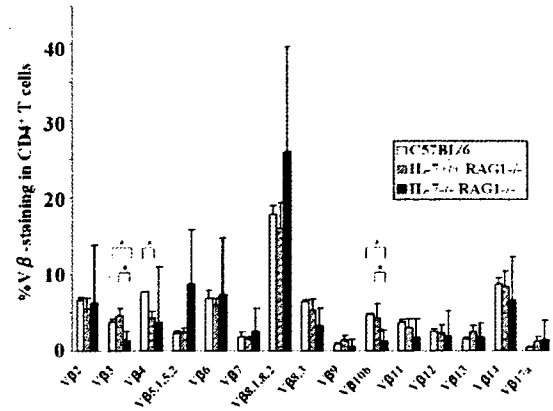

FIGURE 3. Flow cytometric analysis of V families on the surface of the splenic CD4 T cells. To analyze the TCR V family repertoire, splenic cells were double-stained with PE-conjugated anti-CD4 mAb (RM4-5), and the following splenic cells were double-stained with a panel of 15 FITC-conjugated V mAbs. Each percentage value indicates the frequency of each V pooled from three independent experiments (n 12). , p 0.05.

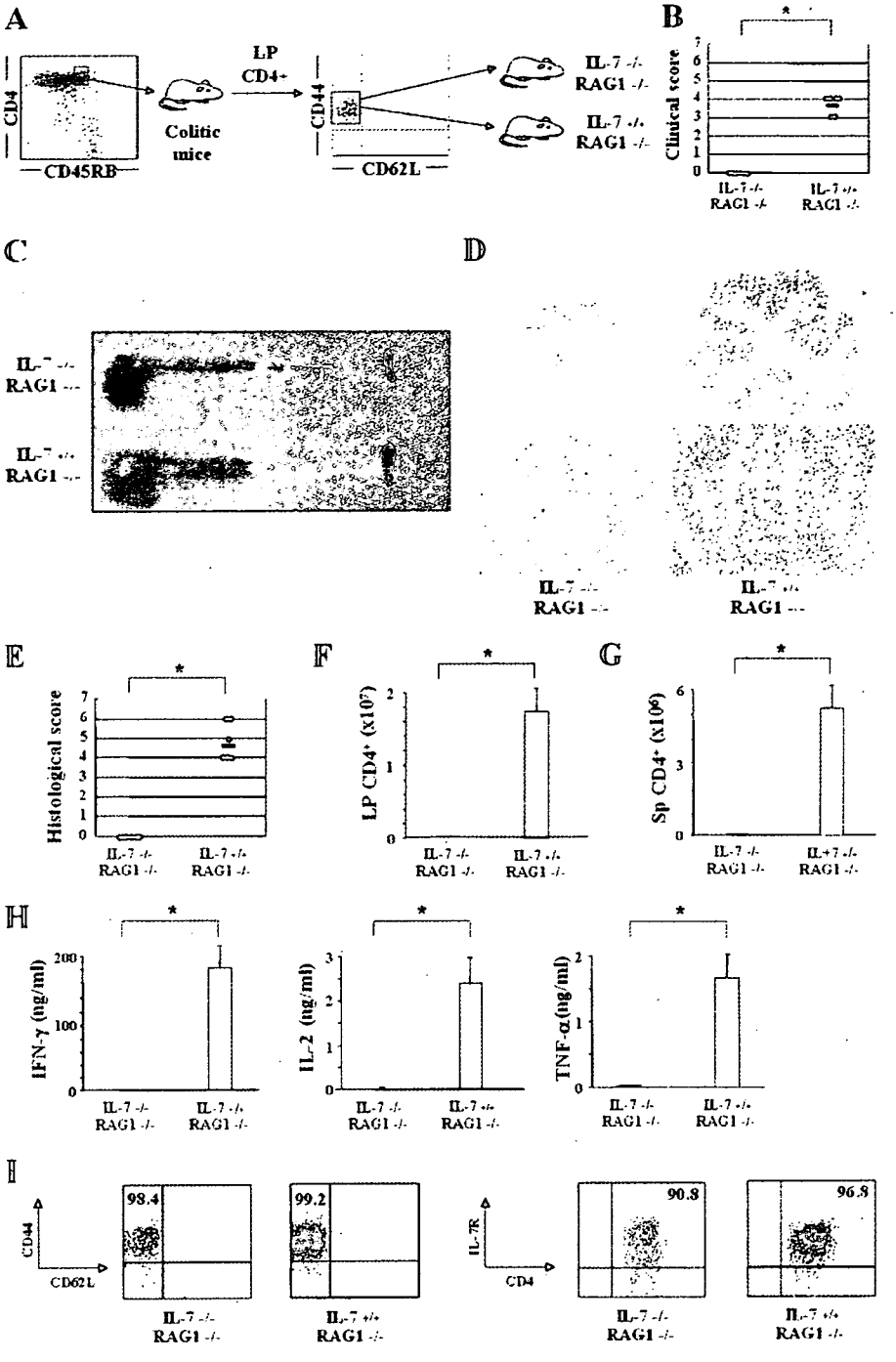

FIGURE 4. IL-7 / RAG-1 / transferred with colitogenic LP CD4 CD44^{high}CD62L T_{EM} cells did not develop chronic colitis. *A*, Colitogenic LP CD4 CD44^{high}CD62L T_{EM} cells obtained from colitic mice transferred with CD4 CD45RB^{high} T cells were transferred into new IL-7 / RAG-1 / (IL-7 / 3 IL-7 / ; *n* 10) and IL-7 / RAG-1 / (IL-7 / 3 IL-7 / ; *n* 10) mice. *B*, Clinical scores were determined 4 wk after transfer as described in *Materials and Methods*. Data are indicated as the mean SEM of seven mice in each group. , *p* 0.005. *C*, Gross appearance of the colon, spleen, and mesenteric lymph nodes from IL-7 / 3 IL-7 / (*top*) and IL-7 / 3 IL-7 / (*bottom*) mice 4 wk after transfer. *D*, Histological examination of the colon from IL-7 / 3 IL-7 / and IL-7 / 3 IL-7 / mice 4 wk after transfer. Original magnification: 40 (*upper*); 100 (*lower*). *E*, Histological scoring of IL-7 / 3 IL-7 / and IL-7 / 3 IL-7 / mice 4 wk after transfer. Data are indicated as the mean SEM of seven mice in each group. , *p* 0.005. LP (*F*) and spleen (*G*) CD4 T cells were isolated from IL-7 / 3 IL-7 / and IL-7 / 3 IL-7 / mice 4 wk after transfer, and the number of CD4 cells was determined by flow cytometry. Data are indicated as the mean SEM of seven mice in each group. , *p* 0.01. *H*, Cytokine production by LP CD4 T cells. CD4 LPL were isolated from each mouse at 4 wk after transfer and stimulated with anti-CD3 and anti-CD28 mAbs for 48 h. IFN- , IL-2, and TNF- concentrations in culture supernatants were measured by ELISA. Data are indicated as the mean SD of seven mice in each group. , *p* 0.005. *I*, Phenotypic characterization of LP CD4 T cells isolated from IL-7 / 3 IL-7 / and IL-7 / 3 IL-7 / mice 4 wk after transfer.

CD4 CD45RB^{high}IL-7R ^{high} naive T cells (0 wk before the transfer), CD4 IL-7R ^{low} effector T cells (1 and 2 wk after the transfer), to CD4 IL-7R ^{high} memory T cells (4 wk after the transfer), suggesting that naive and memory CD4 T cells may be more responsive to IL-7-mediated signaling.

TCR V repertoires in IL-7 / RAG-1 / and IL-7 / RAG-1 / mice transferred with CD4 CD45RB^{high} T cells

Analysis of the TCR repertoire of the immunodeficient SCID/Rag-1/2 / recipients in the CD4 CD45RB^{high} T cell transfer model may provide an opportunity to characterize the unique T cell population present in the diseased individuals in a manner not possible in clinical studies on human patients. Furthermore, it was also possible that the adoptive transfer of CD4 CD45RB^{high} T cells to IL-7 / RAG-1 / recipients gains more skewed and restricted clonality of CD4 T cells as compared with that in IL-7 / RAG-1 / recipients. To assess this possibility, we next made a comparison between TCR V repertoires of splenic CD4 T cells from colitic CD4 CD45RB^{high} T cell-transferred and IL-7 / RAG-1 / and IL-7 / RAG-1 / and normal age-matched wild-type mice. Flow cytometric analysis of these splenic CD4 cells using a panel of 15 anti-V mAbs showed that most major

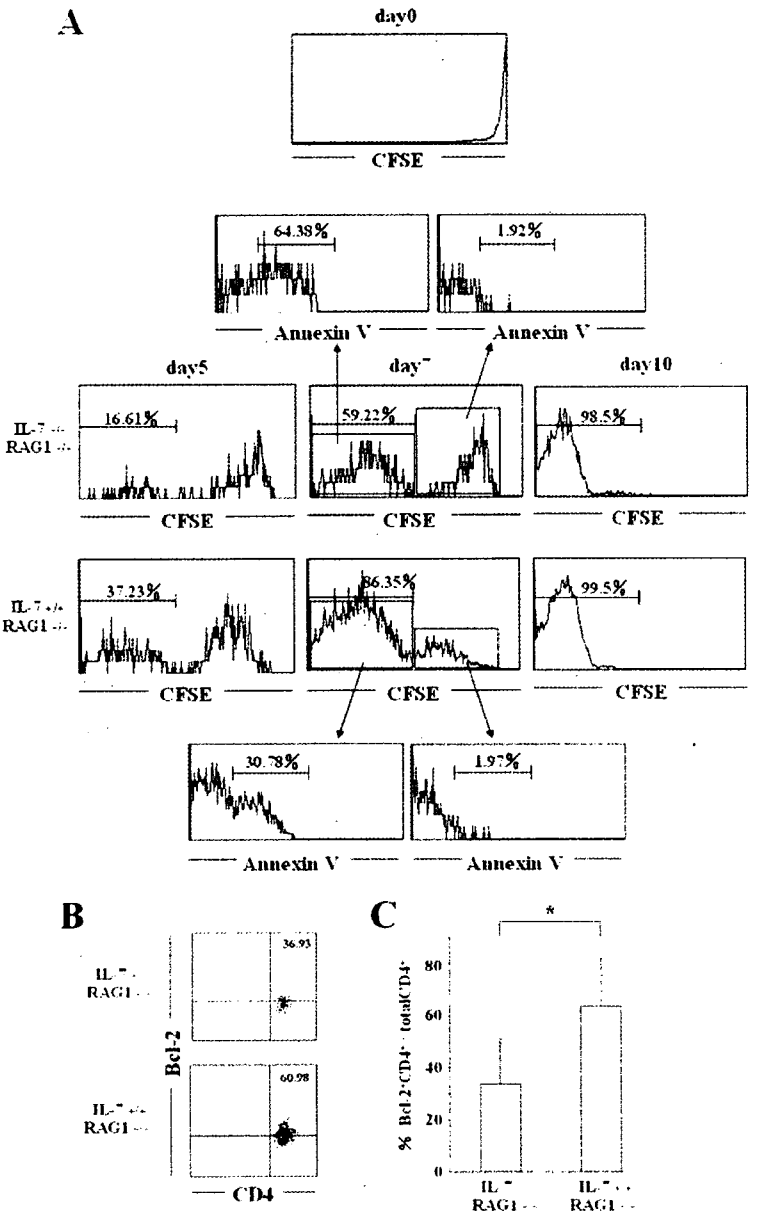

FIGURE 5. IL-7 is essential for the survival, but not the cell turnover, of colitogenic LP CD4 T_{EM} cells. *A*, Colitogenic LP CD4 T_{EM} cells obtained from colitic mice transferred with CD4 CD45RB^{high} T cells were labeled with CFSE and adoptively transferred into IL-7 / RAG-1 / (n 16) or IL-7 / RAG-1 / (n 16) mice. At the indicated time points after transfer (days 4, 8, and 12), CFSE incorporation was determined by flow cytometry. Histograms are gated on CD4 T cells. These data were representative from six experiments. At day 8 after transfer, the gated CFSE cells represent rapid proliferation, and CFSE cells were also stained with annexin V. *B*, Representative flow cytometric histograms showing the expression of Bcl-2 in LP CD4 T cells from IL-7 / RAG-1 / or IL-7 / RAG-1 / mice transferred with the colitogenic LP CD4 T cells 7 days after the transfer. *C*, Average percentage of LP Bcl-2 CD4 T cells from IL-7 / RAG-1 / (n 6) or IL-7 / RAG-1 / (n 6) recipients 7 days after the transfer. , p 0.05.

V population was V 8.1/8.2 in all three groups, i.e., age-matched C57BL/6J and IL-7 / RAG-1 / and IL-7 / RAG-1 / mice transferred with CD4 CD45RB^{high} T cells. Although only a V 4 ratio in colitic IL-7 / RAG-1 / recipients was significantly decreased as compared with that in normal C57BL/6J mice, there were no significant differences of other V repertoires between these two groups (Fig. 3). In noncolitic IL-7 / RAG-1 / recipients, however, the repertoires of V 3 and V 10b were significantly decreased as compared with those in normal C57BL/6J mice and colitic IL-7 / RAG-1 / recipients (Fig. 3), indicating that the lack of IL-7 suppressed the expansion of certain type of V populations as compared with other repertoires.

Lack of colitis in IL-7 / RAG-1 / mice transferred with colitogenic LP CD4 T_{EM} cells

To next assess the role of IL-7 in the persistent colitis without the impact of naive T cell priming, activation, and differentiation, we first isolated LP CD4 T cells as colitogenic CD4 T_{EM} cells from CD4 CD45RB^{high} T cell-transferred colitic RAG-2 / mice at 4–6 wk after transfer because flow cytometry analysis revealed that the colitic LP CD4 T cells were CD44^{high} CD62L IL-7R ^{high} T_{EM} cells (Fig. 1*I*), and we previously demonstrated that the adoptive transfer of these cells into new IL-7-competent RAG-2 / mice induces chronic colitis (17). We then transferred these LP CD4 T_{EM} cells into IL-7 / RAG-1 / mice (IL-7 / 3 IL-7 /) and the IL-7 / RAG-1 / mice (IL-7 / 3 IL-7 /) to focus on the persistence of colitogenic CD4 T_{EM} cells (Fig. 4*A*). IL-7 / 3 IL-7 / recipients developed a severe colitis 4 wk after the transfer, characterized by significant weight loss, diarrhea, and higher total clinical scores (Fig. 4*B*) and thickening of the colonic wall with inflammation (Fig. 4*C*). Average histological scores characterized by transmural inflammation with high numbers of lymphocytes in the LP and submucosa, and prominent epithelial hyperplasia with loss of goblet